JIMMA UNIVERSITY

JIMMA INSTITUTE OF TECHNOLOGY

FACULTY OF MECHANICAL ENGINEERING

DESIGN OF MECHANICAL SYSTEMS STREAM

Title:

Comparative Study of Coil Spring and Air Spring Suspension system on Quarter Car Model

A Research submitted to the Faculty of Mechanical Engineering in Partial Fulfilment of the Requirements for the Degree of Master of Science in Mechanical Engineering.

By: KEYRU SALIA

July, 2021

Jimma, Ethiopia

JIMMA UNIVERSITY

JIMMA INSTITUTE OF TECHNOLOGY

FACULTY OF MECHANICAL ENGINEERING

DESIGN OF MECHANICAL SYSTEMS STREAM

Title:

Comparative Study of Coil Spring and Air Spring Suspension system on Quarter Car Model

A Research submitted to the Faculty of Mechanical Engineering in Partial Fulfilment of the Requirements for the Degree of Master of Science in Mechanical Engineering.

By: KEYRU SALIA

Main Advisor: Dr.-Ing. Mesay Alemu

Co-Advisor: Mr. Fekada Dabalo(MSc)

Declaration

I hereby declare that the work, which is presented in this thesis entitled "**Comparative Study of Coil Spring and Air Spring Suspension system on Quarter Car Model**" is my original work, has not been presented for a degree in any other university, and that all sources of material used for this thesis have been duly acknowledged.

Keyru Salia	_____	_____
	Signature	Date

This thesis has been submitted for examination with our approval.

Dr.-Ing. Mesay Alemu	_____	_____
Main Advisor	Signature	Date
Mr. Fekada Dadalo	_____	_____
Co-Advisor	Signature	Date

Approval

Name: Keyru Salia

Degree: Masters of Science

Title: Comparative Study of Coil Spring and Air Spring Suspension system on Quarter Car Model

Examining Committee:

Main Advisor

Dr.-Ing. Mesay Alemu _____ _____

Signature Date

Co-Advisor

Mr. Fekada Dabalo _____ _____

Signature Date

Chairman

Mr. Iyasu Tafase _____ _____

Signature Date

External Examiner

Dr.-Ing. Getachew Shunki _____ _____

Signature Date

Internal Examiner

Mr. Iyasu Tafase _____ _____

Signature Date

ABSTRACT

Vehicles use suspension systems to attenuate vibrations for the purpose of ensuring Ride Comfort and Road Holding which are contradicting requirements. The degree of their contradiction can be minimized by optimization, employing an active suspension system and using Coil Spring or Air Spring Suspension systems appropriately. Theoretically, Air Spring Suspension systems are better than Coil Spring Suspension systems on high vibration attenuation and less destruction to road. The objective of the research is to compare the performance of Coil Spring Suspension with Air Spring Suspension system through modelling and control of quarter car which is moving with speed of 90 km/h on class-B road. The study gives a numerical figure on the betterment of Air Spring Suspension system over Coil Spring Suspension system. Mathematical model is developed for both systems and simulated in Simulink. The mathematical models are validated with all the correlation coefficients are greater than 0.48. The models are optimized using multi-objective Genetic Algorithm. The optimized Air Spring Suspension system has better Ride Comfort and Road Holding than Coil Spring Suspension system by 1.27% and 0.16% respectively. A Fuzzy Logic Controller is developed and integrated to both systems to show their behaviour when they are applied in active suspension system. The improvement of Ride Comfort in Air Spring Suspension system is more than Coil Spring Suspension system by 3.73%. The design of the air cylinder has to be good enough to prevent heat and pressure losses, because the results of Air Spring Suspension system are obtained based on these considerations.

Keywords

Coil Spring, Air Spring, Suspension system, Ride Comfort, Road Holding, Simulink, Mathematical model, Optimization, Genetic Algorithm and Fuzzy Logic Controller

ACKNOWLEDGMENT

First of all, I am super keen to express my gratitude to **Dr.-Ing Mesay Alemu** for giving me this chance to be my main advisor and his willingness to guide me in conducting the research. Then I am thankful to **Mr. Fekada Dabalo** for his willingness to be my co-advisor and professional supervision.

Next, I would like to appreciate Jimma Institute of technology for giving me the opportunity to continue my education. This is the only way to upgrade one's education level, so career.

Last but not least, my gratitude goes to others who supported me during this study for their valuable support and assistance.

TABLE OF CONTENTS

LIST OF FIGURES

LIST OF TABLES

ACRONYMS

ASS	Air Spring Suspension
CSS	Coil Spring Suspension
DOF	Degree of Freedom
FLC	Fuzzy Logic Controller
GA	Genetic Algorithm
ISO	International Organization for Standardization
LQR	Linear Quadratic Regulator
NB	Negative Big
NM	Negative Medium
NS	Negative Small
NV	Negative Very Big
PB	Positive Big
PM	Positive Medium
PID	Proportional Integral Derivative
PS	Positive Small
PSD	Power Spectral Density
PSO	Particle Swarm Optimization
PV	Positive Very Big
RC	Ride Comfort
RH	Road Holding
RMS	Root Mean Square
ZE	Zero

LIST OF SYMBOLS

A	Cross-sectional Area of air cylinder
r	Radius of air cylinder
P	Pressure in the air cylinder
P_o	Initial pressure of air cylinder
P_{at}	Atmospheric pressure
V	Volume of the air cylinder
V_o	Initial volume of air cylinder
V_{at}	Volume of air cylinder at atmospheric pressure
h_o	Initial height of air cylinder
x	Change in height of air cylinder
T	Temperature in the air cylinder
Q	Heat energy
W	Work done on the system
m	Mass of air in the air cylinder
C_v	Heat capacity of air at constant volume
C_p	Heat capacity of air at constant pressure
R	Difference in specific heats of air
γ	Ratio of specific heats
F_s	Air spring force
F_{so}	Static air spring force
F_{ds}	Dynamic air spring force
K_a	Air spring stiffness
K_{ao}	Air spring static stiffness
K_c	Coil spring static stiffness

K_t	Tyre stiffness
C	Damping coefficient
$\ddot{y}_s$	Sprung mass acceleration
$\dot{y}_s$	Sprung mass velocity
y_s	Sprung mass displacement
$\ddot{y}_u$	Unsprung mass acceleration
$\dot{y}_u$	Unsprung mass velocity
y_u	Unsprung mass displacement
y_o	Road input
m_s	Sprung mass
m_u	Unsprung mass
F_y	Force in vertical direction
r_p	Pearson's Correlation coefficient
h	Height of road input
f	Frequency of road irregularities
t	Time
T_p	Period of oscillation
G_r	Road spectral density
n	Spatial frequency
n_o	Initial spatial frequency
w	White noise signal
v	Vehicle speed
G	Road roughness coefficient
Ω	Angular spatial frequency
Ω_o	Initial angular spatial frequency
a_{RMS}	RMS of sprung mass acceleration
td_{RMS}	RMS of tyre deflection
sw_{RMS}	RMS of suspension working space
F_a	Actuating force

CHAPTER 1

INTRODUCTION

1.1 Background

Vibrations in mechanical components have two effects: either negative or positive. In fact most of the vibrations are unwanted due to their negative effect which leads to catastrophic situations.

Vehicles are transportation media composed of numerous moving mechanical parts. They are highly subjected to negative effects of vibrations caused by different reasons [1]. The causes of the vibrations are: road irregularities, aerodynamic forces, vibrations of the engine and drive line, inertia forces created by the driver's manoeuvres and non-uniformity of the wheel assembly [1–6].

Vehicle vibration affects passenger or driver as a passive vibration movement through the abdominal wall causes hypertension, back pain, osteoarthritis, slipping disc [3, 7]. It also causes damage to different vehicle components. The instability problem which results in danger is due to vehicle vibration as well.

To alleviate these problems suspension system is assembled to a vehicle. Suspension system is a medium which connects sprung mass with unsprung mass. It is used to support the vehicle weight, provide Road Holding(RH), reduce transient force to the body, gives Ride Comfort(RC), and enhance vehicle manoeuvrability [6]. Weight support is done by redistributing the forces exchanged between the tyres and road, thus ensuring the general RH of the vehicle itself and smooth ride gives passengers comfort by filtering, as far as possible, the road irregularities [8].

Two broad categories of suspension system can be employed in vehicles. These are

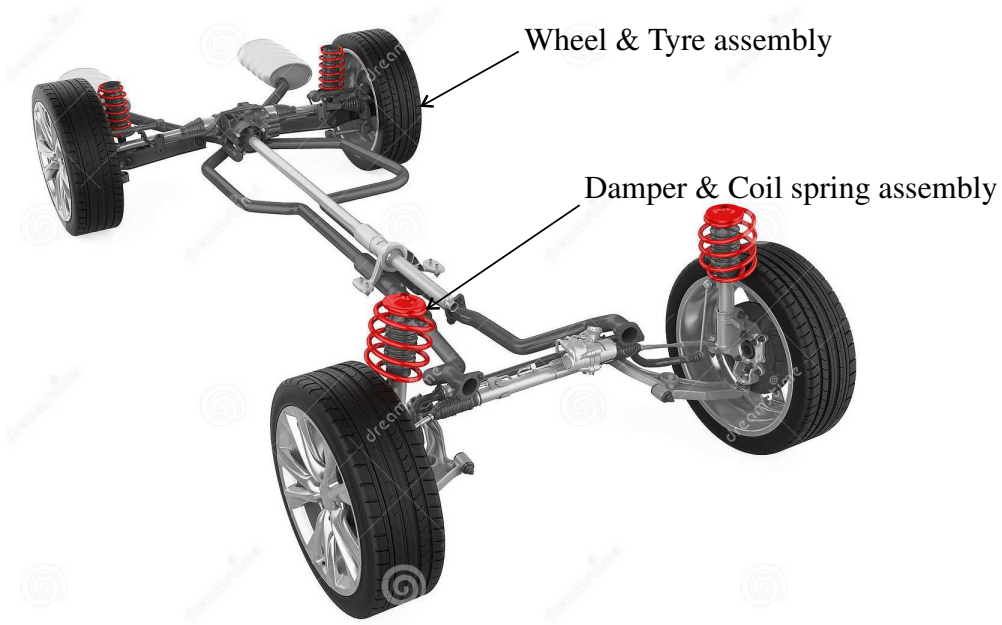

Figure 1.1: Components of CSS system

Coil Spring Suspension(CSS) system and Air Spring Suspension(ASS) system. In CSS system coil springs are used between vehicle body and tyre axle. These springs are compression springs which are subjected to compressive loads due to vehicle dead weight and other dynamic forces. The typical components of CSS systems are shown in Figure 1.1. In most ASS systems air bellow, air lines, valves and other accessories are used to replace coil springs and dampers which are used in CSS system. Figure 1.2 gives the components of ASS system. The design of ASS system may varies due to the arrangement of its components.

In this study only the coil spring in CSS system is replaced by air cylinder with a piston compressed to the required initial pressure. This air cylinder acts as a compression spring because it absorbs the dynamic force of the vehicle by compression of the air inside and releases it back by expansion to some level.

Quarter car suspensions are the most familiar models for the purpose of analysis. They are used to simply study the response of the vehicle at different input conditions. It is used to study not just the responses but also the effect of different suspension parameters, non-linearities, optimization and controllers on vehicle performance. The illustration of quarter car is shown in Figure 1.3 which includes suspension spring, damper/shock absorber and tyre.

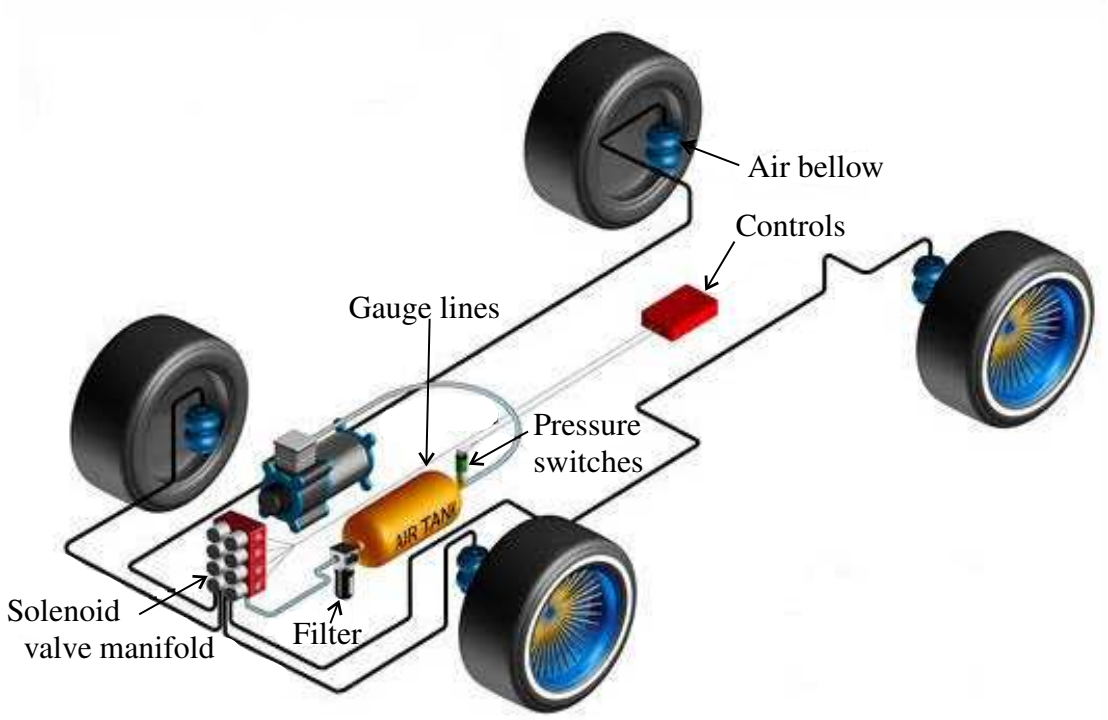

Figure 1.2: Components of ASS system

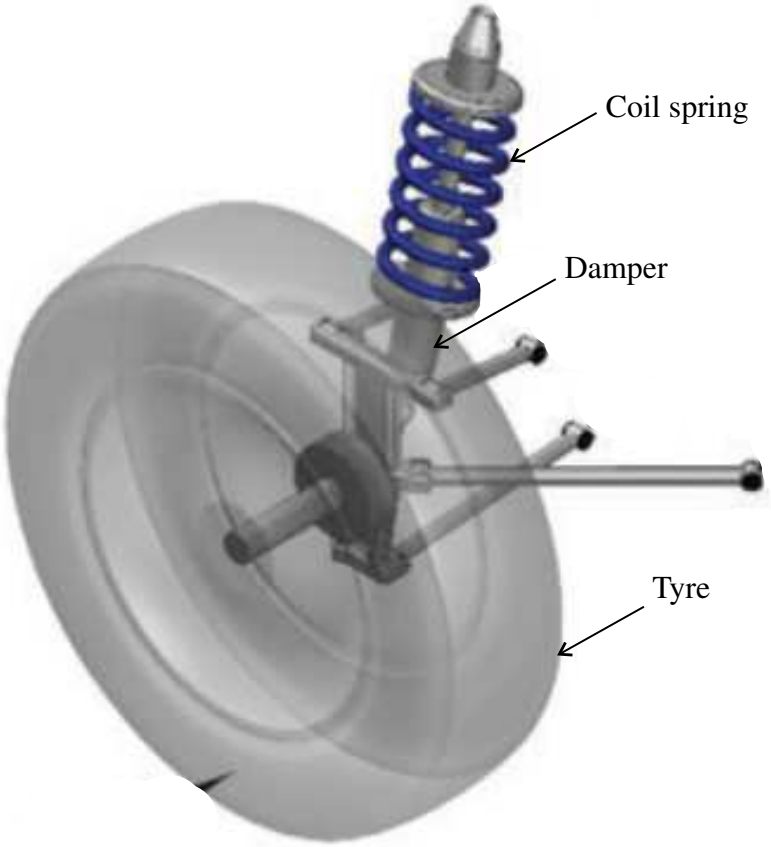

Figure 1.3: Main parts of quarter car suspension system

1.2 Statement of the Problem

Suspension system is an important unit of a vehicle that is responsible for supporting the weight of the vehicle. It attenuates the vibrations in order to provide RC, RH and prevent accident. Poor suspension system design may not give the intended function properly and simultaneously. CSS & ASS systems are commonly used in vehicles. Each of them has the ability to attenuate vibrations. The nature of their action on vehicle performance varies and it is difficult to select the best for specific vehicle. This is because their performance varies on different parameters. Even though different researches explain that ASS systems are better than CSS systems, this is a qualitative comparison. So there must be a quantitative comparison between the performance of ASS and CSS system. This comparison gives a numerical figure on the betterment of ASS system over CSS system

1.3 Motivation

Vehicles hold the majority of ground transport. All these vehicles need a suspension system to isolate the vibrations caused by different reason from the vehicle body. Today luxurious vehicles are emerging in different part of the world. Their quality is measured by the design of the suspension system they have in addition to other criteria. So suspension system must be designed, improved and optimized every time to respond for the highly advancing and changing technological world. Vehicles with ASS system can be designed with adjustable height and have high vibration absorption. This makes the comparison of CSS and ASS system for RC and RH so interesting. In this thesis the comparison is done after multi-objective optimization and employment of FLC to both models.

1.4 Objective

The objective of the study is to compare the performance of CSS with ASS system through Modelling, Optimization and FLC Control of a quarter car using MATLAB/Simulink.

1.4.1 Specific objectives

The specific objectives of this study are;

- To develop and validate a mathematical model of quarter car for both CSS and ASS system
- To optimize the mathematical models by multi-objective GA using MATLAB
- To develop a FLC for the models using MATLAB

1.5 Scope of the study

The research work will cover comparison of the performance of CSS system with ASS system of a light-duty quarter car model in time domain analysis. A linear mathematical model is developed for both systems. Since the performance of each system varies with different parameters, optimized model is used for the study. Because of this, parameter optimization will be applied to the mathematical models. The optimization is done by multi-objective Genetic Algorithm optimization technique. All the simulations of the performance of the two systems for original and optimized model is done in MATLAB/Simulink. The variation of RC and RH with varying sprung mass is shown for both systems. Finally, Fuzzy Logic Controller is developed in MATLAB to demonstrate how the systems behave when they are used in active suspension system. The comparative results of CSS and ASS systems for optimized and active suspension system is also provided. The research will not include cost analysis.

1.6 Significance of the study

The research work will reveal the reason for selecting an appropriate suspension system. It will help automotive companies to upgrade their design according to the need of their customer. Ultimately, it will safeguard human wellness and reduce the chance of accident as of poorly designed suspension system can not absorb the

vibration sufficiently and results in danger. Damages on vehicle components and road deterioration are also minimized by employing appropriate suspension system.

1.7 Methodology

For the purpose of attaining the objective of the research mathematical modelling of ASS and CSS systems is the first task after literature survey. the models are validated and then optimized. Then after a fuzzy Logic Controller is designed and integrated to both systems to show the response of both CSS and ASS systems. The flow chart of the methodology is given in Figure 1.4.

1.8 Structure of the Thesis

This thesis paper is organized in to seven chapters. A brief description of each chapter is given as follows:

As usual chapter one is the starting point of the paper and chapter two presents a literature survey on CSS and ASS systems. different research works conducted on both systems from 2-DOF to 14-DOF are presented here. the important features of active suspension systems and some control methodologies including Fuzzy Logic Controller are also presented at a glance.

Chapter three gives the mathematical modelling, simulation in MATLAB/Simulink and validation of CSS and ASS systems. Chapter four is about the optimization of mathematical models by multi-objective Genetic Algorithm. The optimized models are also simulated in MATLAB/Simulink.

In chapter five Fuzzy Logic Controller is developed and integrated to optimized models of CSS and ASS systems. The response of both CSS and ASS systems to Fuzzy Logic Controller is also shown here by simulation in MATLAB/Simulink. Chapter six provides the comparative results of all the simulations of CSS and ASS systems with their brief discussion. Finally, conclusion, future works and recommendations are given in chapter seven.

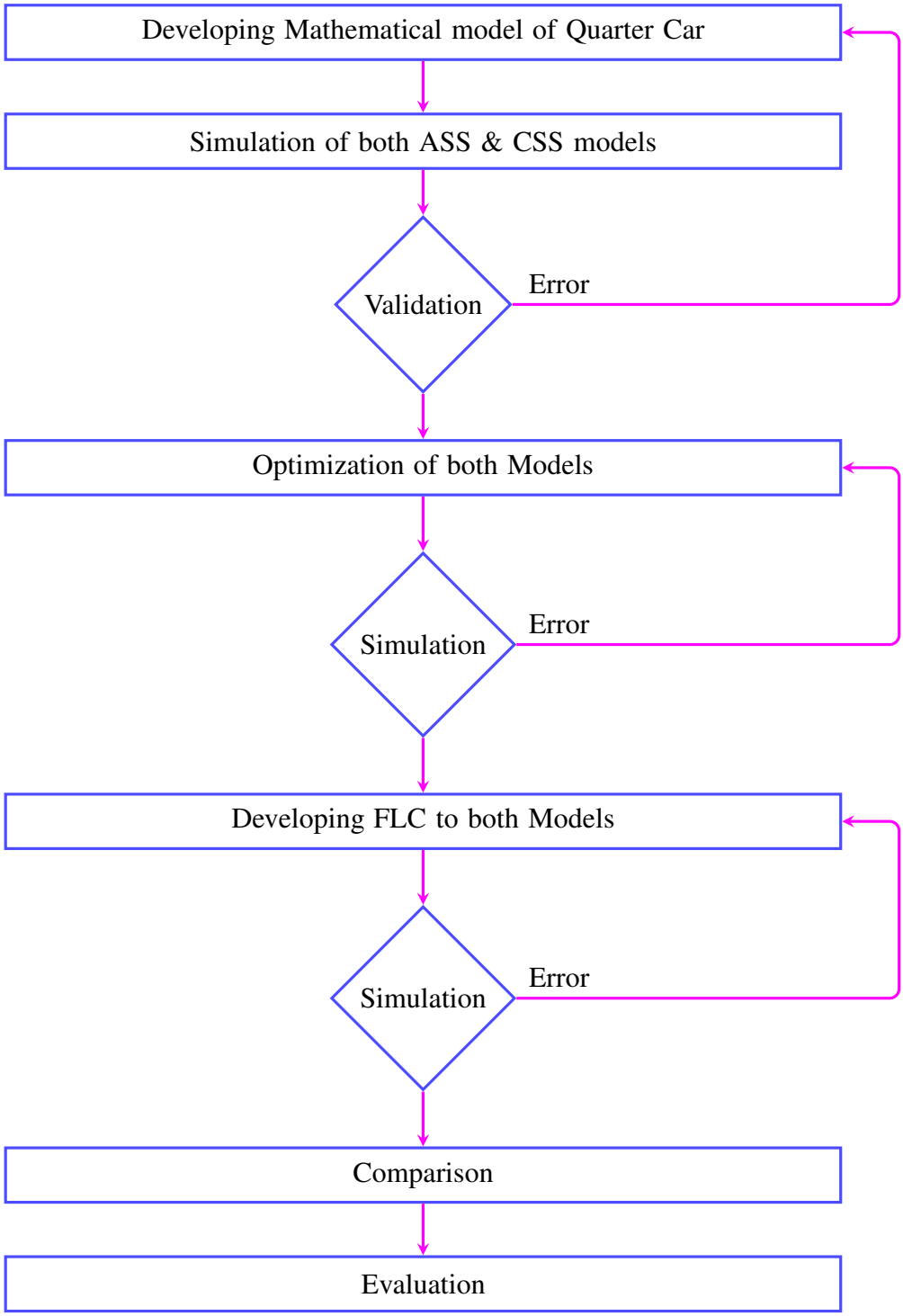

Figure 1.4: Methodology

CHAPTER 2

LITERATURE REVIEW

Present automotive companies are in neck to neck fight with other competitive automotive companies so as to produce a vehicle with better performance. One of the factor that fulfils the performance requirement is advanced suspension system. A suspension system is expected to give better RC and good RH capability. RC is due to low vibration transmissibility and RH is due to low suspension deflection transmissibility of a good suspension system [9]. Unfortunately, achieving RC and RH simultaneously is difficult because they are contradicting requirements [2, 9]. RC principally depends on vertical RMS acceleration value, suspension travel and the frequency of vibrations acted on the body [2, 3, 9] and RH is related to the relative movement between road input and wheel displacement [1].

2.1 Researches on CSS system

For today's vehicle, RC, RH and dynamic control are crucial criteria for customers and also for the selection of an appropriate vehicle [4]. The success of improving vehicle RC and RH is determined by accurate modelling and designing an appropriate control [10].

Kruczek and Stibrsky [11] developed a full car model from four identical quarter car models. They studied vehicle performances during braking, accelerating and steering. In these conditions they discovered that vehicle body roll and pitch cause centre of gravity movement which results in vehicle instability. They also discovered that the side force acting on the wheels depends on tyres, road condition and car speed during steering.

Qiu [7] used quarter car 2-DOF model, to study the ride performance by considering the variations of spring stiffness, damping coefficient and road excitations.

Mitra and Benerjee [3] developed 4-DOF quarter car model with seating on a cushion seat to study the effect of variation of spring stiffness and damping coefficient on RC, RH and human-head displacement. Simulation is done using Bond graph and Simulink model for validation. They described the effect of road irregularities, car speed, and variation of spring stiffness and damping coefficient on RC, RH and human-head displacement. They found that, RC decreases as speed increases up to 10 km/h and then increases for stiffer bump width up to 2 m. RC also increase with increase in damping coefficient up to 1500 Ns/m and then decreases slightly. RH decreases with increase in car speed and spring stiffness.

Mitra *et al.* [1] developed a detailed analytical formation of the governing equation of a full car 7-DOF model and used Simulink 7-DOF model for validation. In this study it is stated that for the proper RH relative displacement between the wheel and road must be in the range of 0.0508 m. It is also found that the effect of bump of same amplitude nearly has no effect on pitch angle and roll angle of the vehicle.

Zehsaz *et al.* [4] modelled the dynamic behaviour of an off-road vehicle with a system of 7-DOF to indicate the effect of spring stiffness and damping coefficient variation on RC. He showed that RC is more sensitive to rear damping coefficient change and increases with increase in mass on the rear suspension system and decrease in spring stiffness. RC also increases by different combination of spring stiffness and damping coefficient with a cost of RH. During acceleration, due to the shift of load to the rear wheel, the equivalent load at the rear increases and then the RC increases.

Mitra *et al.* [2] developed quarter car model in MSC-ADAMS and validated experimentally by building a quarter car test rig. This study obtains RC by varying sprung mass, unsprung mass, tyre pressure, car speed, spring stiffness, damping coefficient, camber angle and toe distance. RC decreases when spring stiffness increases at constant damping coefficient and when damping coefficient increases at constant spring stiffness. Inflation pressure affects moment characteristics, tyre force, load radius and spring rate.

Since a suspension system supposed to give contradicting requirements, there must be an optimization or an active suspension system must be employed. Optimizations have

little improvement by giving the appropriate configuration of vehicle parameters. In addition to optimization controllers have to be used to achieve the contradicting requirements at high level. Natural frequency of passive suspension system is more than active suspension system [5]. Active suspensions have the ability to fully counteract the manoeuvring-induced loads to the suspension and the ability to provide significant vehicle body damping without adverse effects over passive suspensions [6]. Darus *et al.* [12] use LQR controller for a full car active suspension system to improve ride quality. But LQR controller cannot perform well in rough road especially for full car model. Demir *et al.* [10] applied a Fuzzy logic controller to a non-linear half car model and compared with a PID controller. They finally developed a hybrid PID-Fuzzy logic controller. Fuzzy logic controller can cope the non-linearities in vehicle suspension and it doesn't depend on the accuracy of the mathematical model.

2.2 Researches on ASS system

Currently, ASS systems got more applicability than CSS systems due to their ability to give better RC, RH, safety, less destruction to road and height control [13, 14]. They have lower natural frequency, low vibration transmissibility, variable spring rate with constant natural frequency and adjustable carrying capacity [14, 15].

Lee [16] derived a mathematical model of an air spring using energy conservation law. The model is validated experimentally. In this study, volume variation, heat transfer, air mass variation and effective area have a direct effect on the stiffness of air spring.

Toyofuku *et al.* [13] developed a mathematical model of ASS system with auxiliary chamber. The auxiliary chambers and pipes are used to change spring constant in controlling condition. The study reveals that the effect of auxiliary chamber at high frequencies is minimum, which is due to the inertia of the air in the pipe not the friction.

Li *et al.* [17] established a single DOF mathematical model of ASS system with auxiliary chamber by using the theory of aerodynamics, Engineering thermodynamics and fluid mechanics to study its damping characteristics. It is found that maximum damping ratio corresponds to larger diameter of the throttle valve.

Narayan *et al.* [18] introduce a hybrid design of coil spring and Air bladder design for

better RC and stability.

Prassad and Mohan [9] applied LQR control design to a dynamic quarter car model of an ASS system and compared it with PID control design. This work improves RC by reducing maximum displacement amplitude and settling time. Increase in fixed volume and area results an increase in air mass flow rate of ASS system which has a positive effect on car stability.

Akpakpavi and Jiang [14] developed a laterally interconnected ASS system. This study reveals that lateral interconnection decreases roll stiffness of ASS significantly which implies the body rolling moment in turning condition is deteriorated.

Zhu *et al.* [15] developed a mathematical model for a pneumatically pitch-interconnected ASS system. These systems can suppress the car pitch vibration without affecting its bounce properties. This study shows pneumato-dominated frequency decreases and the resonance frequency amplitude increases as the pipe length increases, the reverse is true for pipe diameter.

Quaglia *et al.* [8] conducted a study on the comparison of ASS system with by-pass resistance and fixed auxiliary volume and he found that ASS system with a by-pass resistance is advantageous over the ASS system with a fixed volume in term of DOF.

Le [19] developed a new ASS model of 14-DOF and compared it with the ordinary ASS model. This study considers volume, temperature, mass flow rate, density and energy of the air.

Moheyeldein [20] used quarter car analytical model to compare the performance of ASS system with passive suspension system. The comparison is based on body acceleration, suspension travel and dynamic tyre load. Pressure increment above some level hurts the performance of ASS system.

2.3 Literature Summary

- RC is related to RMS of sprung mass acceleration and RH is related to RMS of tyre deflection
- Spring stiffness, damping coefficient, inflation pressure, car speed, acceleration, deceleration and steering affect RC and RH

- ASS systems can be laterally interconnected, pneumatically pitch-interconnected or unconnected between the wheels
- In ASS system, RC and RH are affected by length of air line, cross-sectional area of air line, height of air bellow(auxiliary volume) and the use of fixed auxiliary volume or a reservoir with a by-pass resistance in addition to vehicle motion parameters
- ASS systems have high vibration attenuation and less destruction to road
- Active suspension systems are used to avoid low frequency body bouncing or extra high frequency harshness than passive suspension systems

2.4 Research Gaps

- The nature of RC and RH with increasing sprung mass is not studied
- The performance of ASS and CSS system is not compared clearly
- The effect of back/front excitation on front/back wheel is not studied
- Most of the studies assume that full car model is obtained from four quarter car models which are connected by solid rod. This assumption is not valid because in most suspension systems all the four wheels are independent of one another or the front wheels are independent of the rear wheels and vice versa. Even the influence of one wheel on the other is not considered and validated

CHAPTER 3
MATHEMATICAL MODELLING

In this chapter a mathematical model for ASS and CSS system is developed and simulated in MATLAB/Simulink. the air spring is modelled on the bases of thermodynamic system and its spring nature is validated. The mathematical model of CSS system is also validated.

3.1 Introduction

Mathematical models are equations which relate the input-output behaviour of a system. The basis for any mathematical model is the fundamental physical laws that govern the system. Mathematical modelling is the process of representing the behaviour of a real system by a collection of mathematical equations and logic which shows input-output relationship. It is used to forecast the nature of the system without having the real action. This could be done through computer simulation.

Almost all vibrating systems have complexities in modelling, and it is impossible to consider the full nature of the systems for mathematical modelling. Often the most important features are considered in mathematical modelling for the analysis to predict the behaviour of the system under specified input conditions and the overall behaviour of the system can be determined by considering even a simple model of the complex system.

2-DOF quarter car models, which are subjected to road excitation, are the simplified form of full car for the purpose of analysis. They are commonly employed in many areas of the automotive industry. The mathematical model of a quarter car suspension system

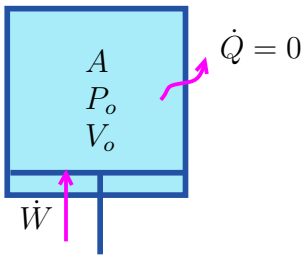

Figure 3.1: Simple thermodynamic closed system

consists of basic elements of the suspension system such as sprung mass (representing chassis), unsprung mass(representing wheel assembly and axle), damping coefficient, tyre stiffness and suspension stiffness. The suspension stiffness is a non-linear function of cross-sectional area, volume, pressure of the air cylinder and suspension deflection for the case of ASS system.

3.2 Mathematical modelling of ASS system

The mathematical model of air spring is developed based on thermodynamic systems. Thermodynamic system can be open or closed system. Open system undergoes mass and energy transfer with its surrounding while closed system not. The air spring used in this study is assumed to be closed system which is an air cylinder, Figure 3.1. It has a constant cross-sectional area (A), initial volume (V_o) and initial pressure (P_o). The volume of the cylinder varies with the displacement of the piston (x). The air cylinder doesn't permit any heat transfer to the surrounding. A piston is provider to compress the air inside the air cylinder which doesn't permit the transfer of mass to the surrounding. Piston rod is used to mount the air cylinder to the vehicle body. An external work is done on the air cylinder by the vehicle static and dynamic forces.

From first law of thermodynamics,

$$dQ + dW = dU \tag{3.1}$$

Since the system is assumed to be adiabatic closed system, $dQ = 0$ & $dm = 0$.

Thus,

$$dW = dU \tag{3.2}$$

But

$$dW = PdV \tag{3.3}$$

&

$$dU = C_v dT \tag{3.4}$$

Then Equation 3.2 becomes,

$$PdV = C_v dT \tag{3.5}$$

Air can be assumed to be ideal gas and the ideal gas equation is;

$$PV = mRT \tag{3.6}$$

Taking derivative on both sides;

$$PdV + VdP = mRdT \tag{3.7}$$

From Equations 3.5 & 3.7, solving for dT gives;

$$dT = \frac{PdV}{c_v} \tag{3.8}$$

&

$$dT = \frac{PdV + VdP}{mR} \tag{3.9}$$

Combining Equation 3.8 and Equation 3.9 gives;

$$(C_v + mR)\, PdV + C_v VdP = 0 \tag{3.10}$$

But

$$C_v + mR = C_p \tag{3.11}$$

Then

$$\frac{C_p PdV}{C_v} + \frac{C_v VdP}{C_v} = 0 \tag{3.12}$$

Substituting $\frac{C_p}{C_v} = \gamma$,

$$\frac{dP}{P} = -\gamma \frac{dV}{V} \tag{3.13}$$

Integrating on both sides from initial points to final points,

$$P = P_o\left(\frac{V_o}{V}\right)^{\gamma} \tag{3.14}$$

3.2.1 Air Spring Force

An external force is acting on the air cylinder through and external work. The force acting on the air cylinder is the product of internal pressure and cross-sectional area of the air cylinder. Thus, the total spring force (F_s), which is the sum of static force (F_{so}) and dynamic force (F_{ds}) is

$$F_s = (P - P_{at})\, A \tag{3.15}$$

Solving for F_{so} at P_o,

$$F_{so} = (P_o - P_{at})\, A \tag{3.16}$$

From the definition,

$$F_s = F_{so} + F_{ds} \tag{3.17}$$

From Equation 3.14,

$$P = P_{at}\left(\frac{V_{at}}{V}\right)^{\gamma} \tag{3.18}$$

$$P_o = P_{at}\left(\frac{V_{at}}{V_o}\right)^{\gamma} \tag{3.19}$$

Now, from Equation 3.14, Equation 3.18 and Equation 3.19,

$$F_s = AP_o\left[\left(\frac{V_o}{V_o - Ax}\right)^{\gamma} - \left(\frac{V_o}{V_{at}}\right)\right] \tag{3.20}$$

Solving for F_{so} at $x = 0$,

$$F_{so} = AP_o\left[1 - \left(\frac{V_o}{V_{at}}\right)\right] \tag{3.21}$$

From Equation 3.16,

$$F_{ds} = AP_o\left[\left(\frac{h_o}{h_o - x}\right)^{\gamma} - 1\right] \tag{3.22}$$

3.2.2 Air Spring Stiffness

Stiffness is the resistance of a material to deflection when force is applied on it. The stiffness of the air spring is determined by taking the derivative of spring force with respect to the deflection (x). The deflection is the change in height of the air cylinder.

$$K_a = \frac{dF_s}{dx} \tag{3.23}$$

$$K_a = \frac{\gamma A^2 P_o}{V_o}\left(\frac{h_o}{h_o - x}\right)^{\gamma+1} \tag{3.24}$$

Solving for K_{ao} at $x = 0$,

$$K_{ao} = \frac{\gamma \pi r^2 P_o}{h_o} \tag{3.25}$$

The total force, static force and dynamic force are given as;

$$F_s = \int_{-x_a}^{x} K_a(x)\,dx \tag{3.26}$$

$$F_{so} = \int_{-x_a}^{0} K_a(x)\,dx \tag{3.27}$$

$$F_{ds} = \int_{0}^{x} K_a(x)\,dx \tag{3.28}$$

3.2.3 ASS system dynamic modelling

The mathematical model of ASS system is developed by replacing the coil spring in ordinary CSS system with air spring. The air spring is an air cylinder which should be designed for the purpose of maintaining high internal pressure and no heat loss. The air cylinder has a volume which varies linearly with the change in height of the cylinder as given in Equation 3.29. The change in height of the air cylinder is the difference of sprung mass displacement and unsprung mass displacement which is given in Equation 3.30. The cross-sectional area of the cylinder is assumed constant for this study.

$$x = y_s - y_u \tag{3.29}$$

$$V = V_o - Ax \tag{3.30}$$

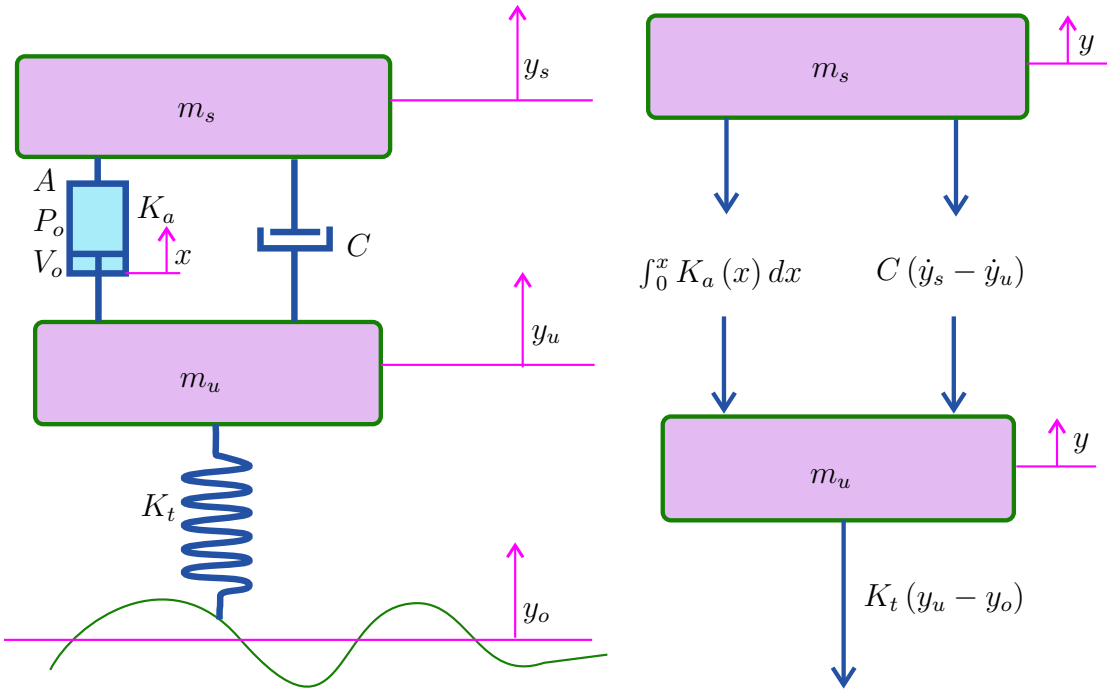

Figure 3.2: Dynamic model and FBD of quarter car ASS system

Figure 3.2 shows an illustrative quarter car model of ASS system on the left with its FBD on the right. It is a 2-DOF system which allows only vertical motion for both sprung mass and unsprung masses. Newton's second law is applied to the masses to get the mathematical model equations. Applying Newton's second low to the free body diagram of sprung mass,

$$\sum F_y = m_s \ddot{y}_s$$

$$m_s\ddot{y}_s + C\left(\dot{y}_s - \dot{y}_u\right) + AP_o\left\{\left[\frac{h_o}{h_o - (y_s - y_u)}\right]^{\gamma} - 1\right\} = 0 \tag{3.31}$$

Applying Newton's second low to the free body diagram of unsprung mass,

$$\sum F_y = m_u \ddot{y}_u$$

$$m_u\ddot{y}_u - C\left(\dot{y}_s - \dot{y}_u\right) - AP_o\left\{\left[\frac{h_o}{h_o - (y_s - y_u)}\right]^{\gamma} - 1\right\} + K_t\left(y_u - y_o\right) = 0 \tag{3.32}$$

3.3 Mathematical modelling of CSS system

The illustrative quarter car model of CSS system is shown in Figure 3.3 at the left with its FBD on the right. Applying Newton's second low to the free body diagram of sprung

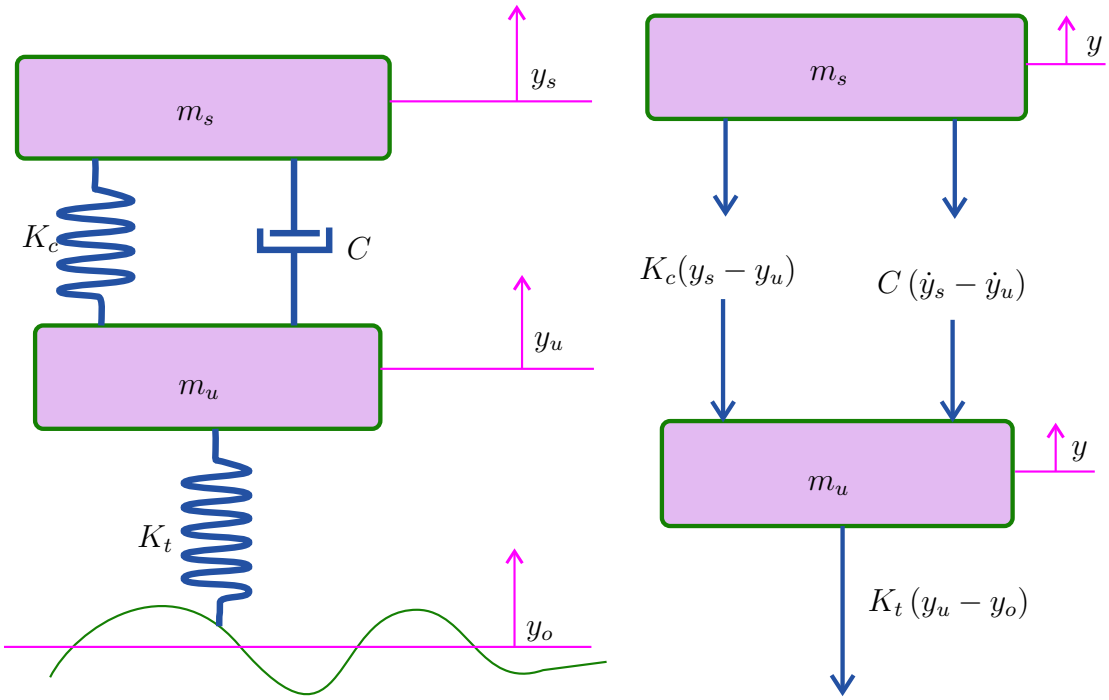

Figure 3.3: Dynamic model and FBD of quarter car CSS system

mass,

$$\sum F_y = m_s \ddot{y}_s$$
$$m_s \ddot{y}_s + C\,(\dot{y}_s - \dot{y}_u) + K_c\,(y_s - y_u) = 0 \tag{3.33}$$

Applying Newton's second low to the free body diagram of unsprung mass,

$$\sum F_y = m_u \ddot{y}_u$$
$$m_u \ddot{y}_u - C\,(\dot{y}_s - \dot{y}_u) - K_c\,(y_s - y_u) + K_t\,(y_u - y_o) = 0 \tag{3.34}$$

3.4 Simulink Model of ASS & CSS system

The above mathematical models are utilized to develop the Simulink model with a given numerical values. In Table 3.1, the numerical data for quarter car model are given from which the data for CSS system are taken from [20].

Table 3.1: Numerical values of quarter car suspension system

Quarter car Parameters	Units	Magnitude
Sprung mass (m_s)	*Kg*	350
Unsprung mass (m_u)	*Kg*	50
Damping coefficient (C)	*N.s/m*	1,500
Tyre stiffness (K_t)	*N/m*	200,000
Coil spring stiffness (K_c)	*N/m*	20,000
Air spring cylinder initial height (h_o)	*m*	0.2884
Air spring cylinder initial pressure (P_o)	*Pa*	600,000
Air spring cylinder cross-sectional area (A)	m^2	0.006867
Specific heat ratio (γ)	-	1.4

3.4.1 Simulink Model of ASS system

The model of ASS system is developed in Simulink for simulation, Figure 3.4. The simulation is run for 3 seconds on step input road with a height of excitation of 0.1 m. The results of simulation are given in combination with CSS system, for sprung mass acceleration, Figure 3.6 and sprung mass displacement, Figure 3.7.

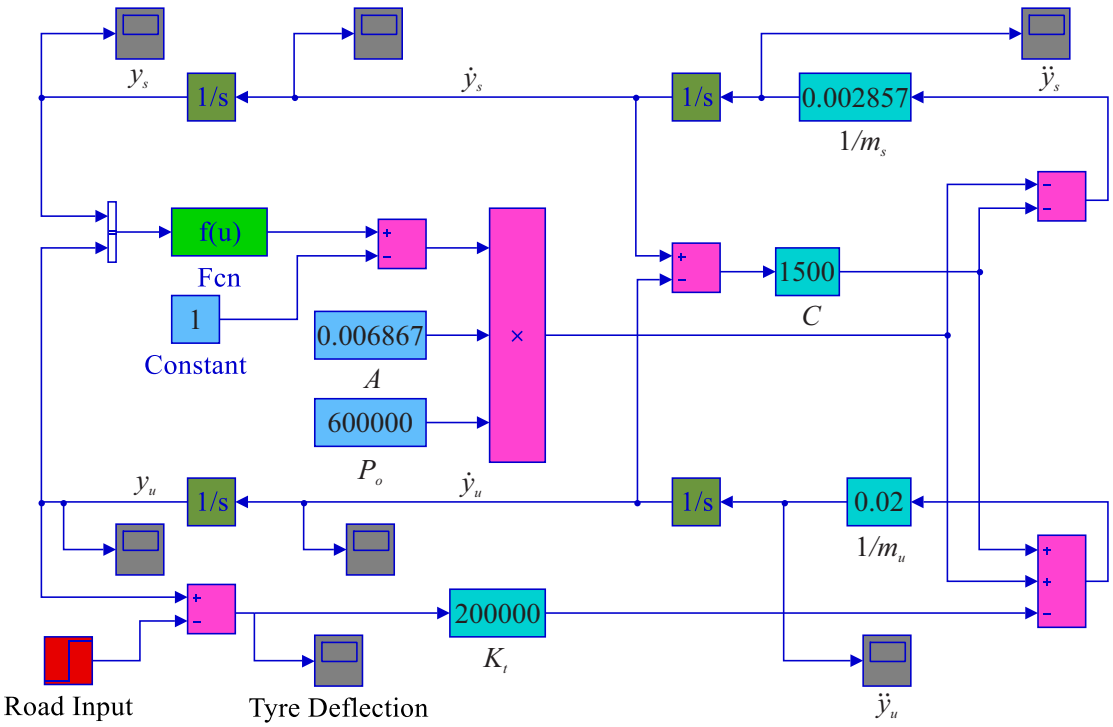

Figure 3.4: Simulink Model of ASS system Quarter Car

3.4.2 Simulink Model of CSS system

The model of CSS system is developed in Simulink for simulation, Figure 3.5. The simulation is run for 3 seconds on Step input on road with a height of excitation of 0.1 m. For both CSS and ASS models, since the input is applied once and kept constant, the sprung mass acceleration reaches its highest value immediately and then tries to diminish rapidly, Figure 3.6. In the same way, the sprung mass displacement gets its highest value and tries to oscillate around the input value, since it is displaced from its original position, Figure 3.7. The amplitude of the oscillation diminishes rapidly.

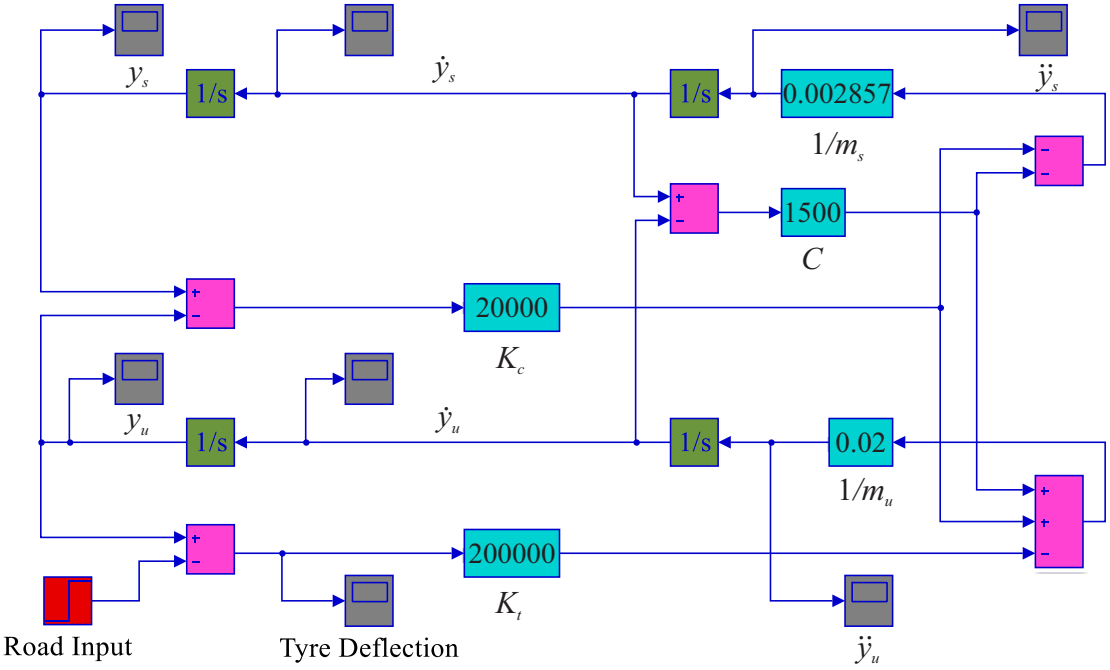

Figure 3.5: Simulink Model of CSS system Quarter Car

3.5 Validation

Validation is checking the agreement of models with the real/laboratory systems. It is used to measure the accuracy of mathematical models.

3.5.1 Validation of Air Spring Model

The validation of air spring model is done by comparing it with the air spring model which is developed and validated by Quaglia *el al.* [8]. This model has a linear

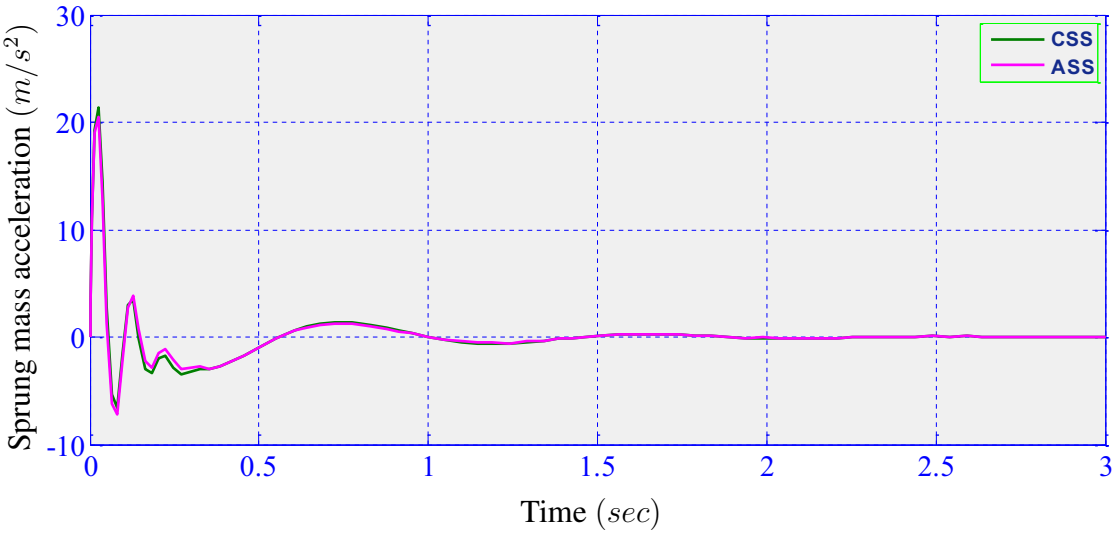

Figure 3.6: Sprung mass Acceleration of CSS and ASS system for Step input

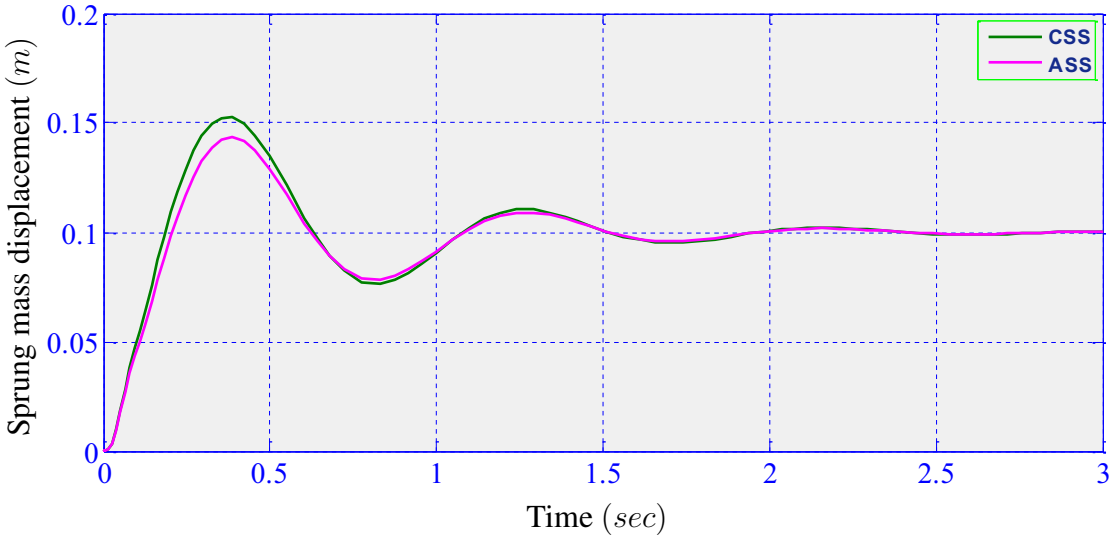

Figure 3.7: Sprung mass displacement of CSS and ASS system for Step input

relationship with the deformation. But the new model has a weaker exponential relationship with the deformation. The graphical representation of both models is shown in Figure 3.8. The coefficient of correlation (r_p) between the plots is 0.9987. This is a guaranty for the accuracy of the model.

3.5.2 Validation of CSS system

The CSS system is simulated in Simulink and validated by comparing the simulation with experimental work which is conducted by Taskin *et al.* [21]. The experimental

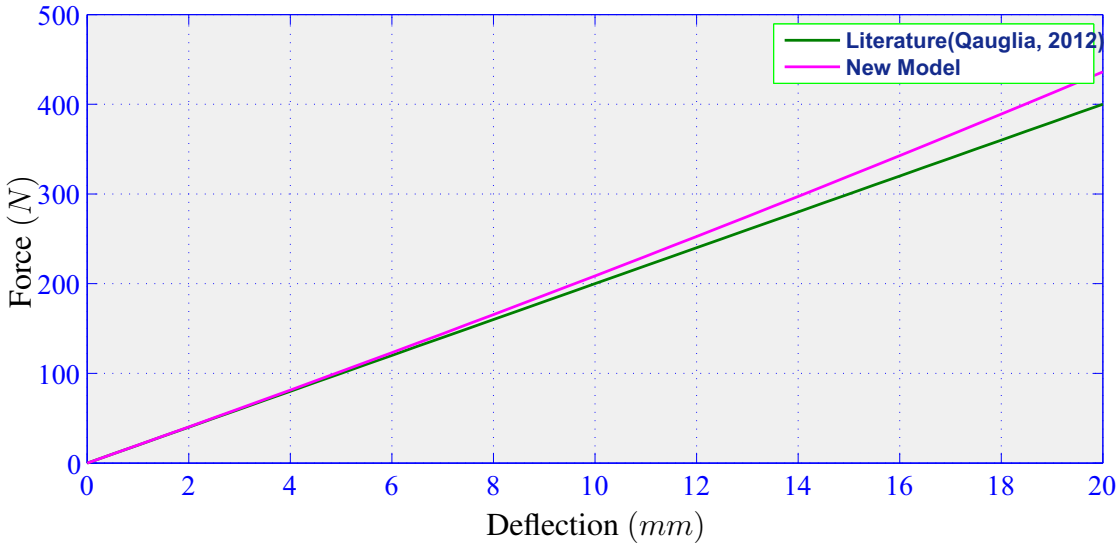

Figure 3.8: Force vs Deflection graph of the New Model and Literature

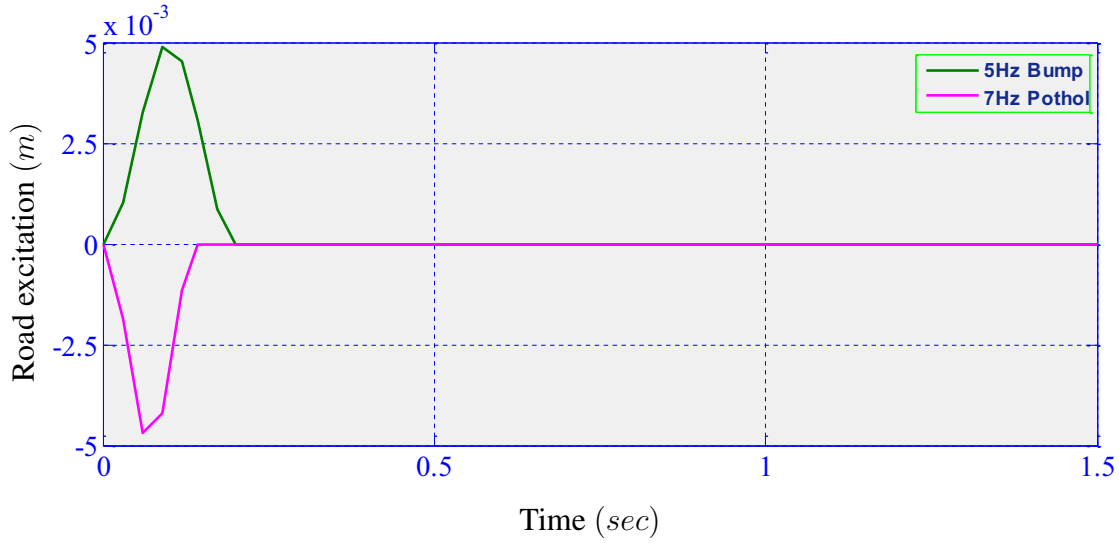

Figure 3.9: Road models used for validation of CSS system

work uses two road models with a height of 0.005 m which are given by Equation 3.35.

$$y_o(t) = \begin{cases} h\left[1 - \cos\left(2\pi f t\right)\right]/2 & ; \quad 0 \leq t \leq T_P \\ 0 & ; \quad otherwise \end{cases} \tag{3.35}$$

Where; h, f, t and T_P are twice of bump height or pothole depth, frequency, time and period of excitation respectively

The two road models are a bump with frequency of 5Hz and pothole with frequency of 7Hz which are shown in Figure 3.9.

The results of simulation and experimental study at each road condition are shown in Figure 3.10 through Figure 3.13 with their respective correlation coefficients (r_p). In

Figure 3.10 the response of sprung mass displacement and in Figure 3.11 the response sprung mass acceleration are given for 5Hz bump of road condition. These Figures have a correlation coefficient of 0.94 and 0.89 respectively, which shows the simulation is much closer to the experimental study.

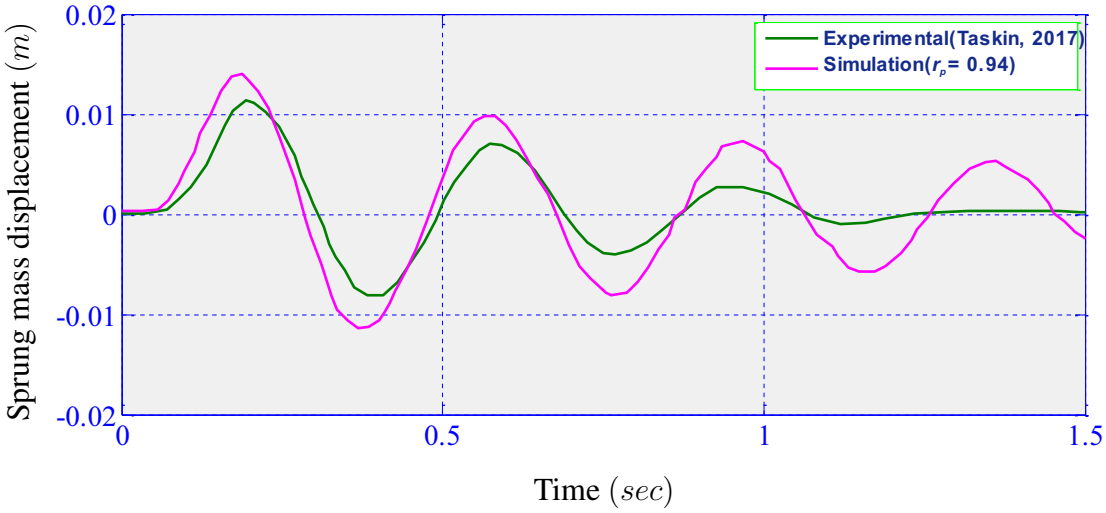

Figure 3.10: Sprung mass displacement of Simulation and Experiment

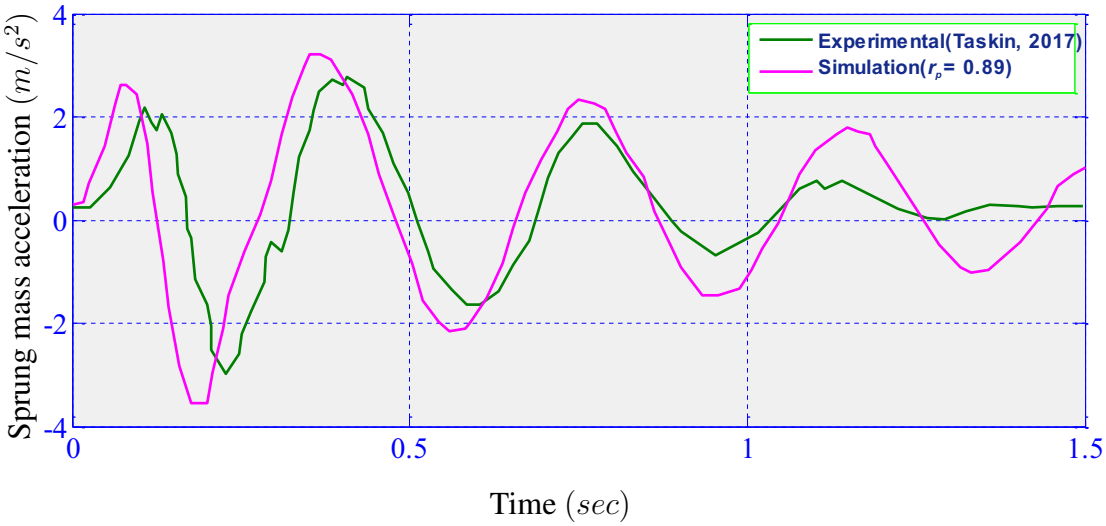

Figure 3.11: Sprung mass acceleration of Simulation and Experiment

In Figure 3.12 the response of sprung mass displacement and in Figure 3.13 the response sprung mass acceleration are given for 7Hz pothole of road condition. Theses Figures have a correlation coefficient of 0.87 and 0.59 respectively, which shows the simulation is much closer to the experimental study.

From all the figures the simulation and experimental results have closer behavioural relationship. The correlation coefficient for all cases is between zero and one which implies the data have a positive relationship. Correlation coefficient of one is the

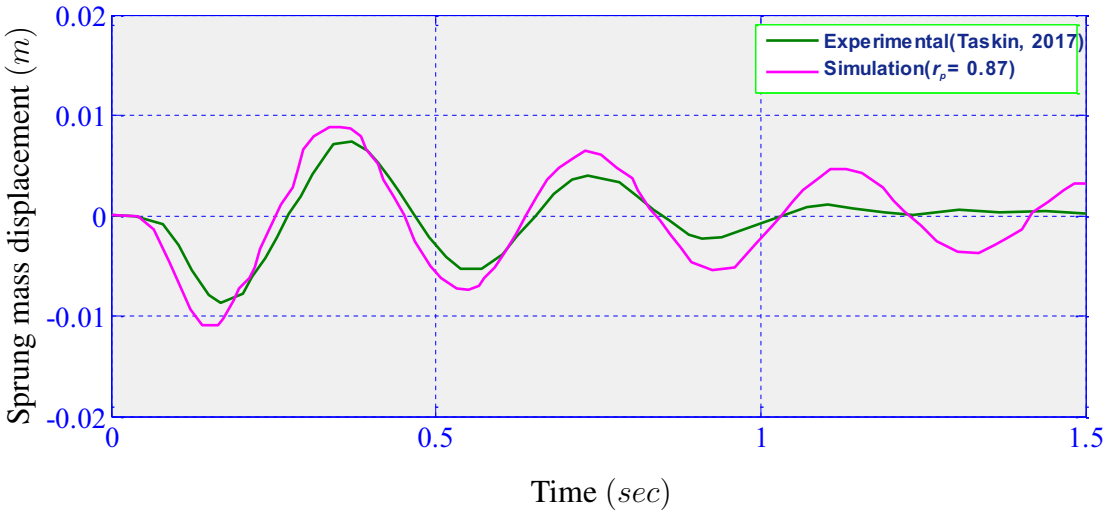

Figure 3.12: Sprung mass displacement of Simulation and Experiment

maximum achievable value for two identical data. The reason for the discrepancy in this work is due to;

- Software limitation
- Consideration of linear system
- Using simplified mathematical model
- The interval of time used for determination of correlation coefficient

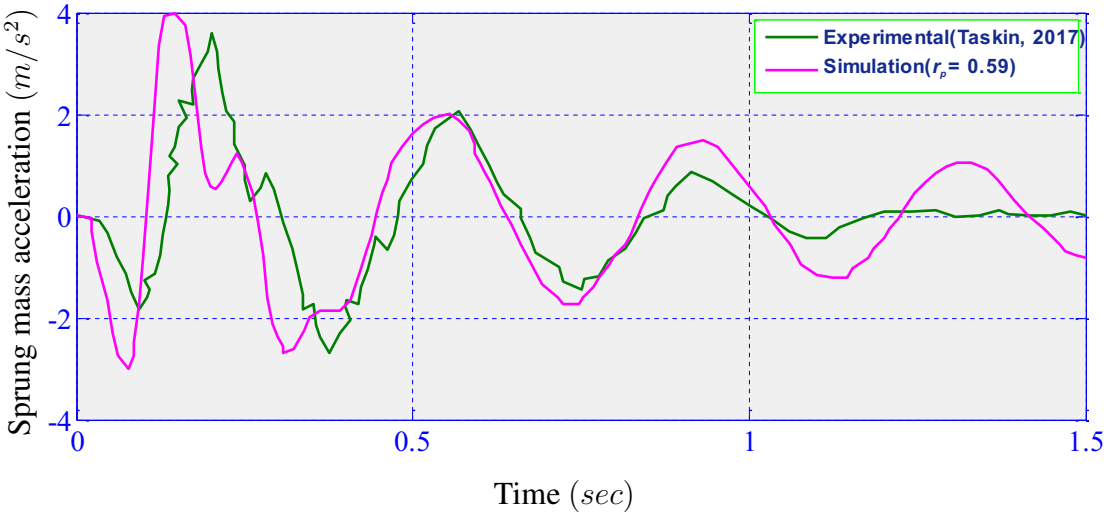

Figure 3.13: Sprung mass acceleration of Simulation and Experiment

CHAPTER 4

OPTIMIZATION

This chapter is all about optimization of the mathematical models of CSS and ASS systems that are developed and validated in chapter three. the optimization technique used is mutli-objective Genetic Algorithm. The optimization is performed on a vehicle which is moving with a speed of 90 km/h (25 m/s) on a class-B road.

4.1 Introduction

Suspension system is supposed to give two conflicting requirements. These requirements are RC and RH. Both requirements vary with different parameters of the suspension system differently and have different combinations at different point. Currently optimization techniques are being employed on vehicle suspension systems to obtain the best configuration of the suspension system variables. Optimization is the act of obtaining the best result under a given circumstances [22]. Genetic Algorithm (GA) is among the many type of optimization techniques which is under the category of modern optimization techniques.

GA is based on the principle of natural genetics and natural selection. The basic elements of natural genetics are performed by three operations as Reproduction, Cross-over and Mutation [22]. GA is general purpose stochastic optimization methods for obtaining global optimum point [23].

Table 4.1: Road degree of roughness as a function of spacial frequency

Road Class	Degree of roughness		
	Lower limit	Geometric mean	Upper limit
	Spatial frequency units, n $G_r(n_o) \times 10^{-6} m^3$		
A	-	16	32
B	32	64	128
C	128	256	512
D	512	1,024	2,048
E	2,048	4,094	8,192
F	8,192	16,384	32,768
G	32,768	65,536	131,072
H	131,072	262,144	-

4.2 Road Modelling

Road irregularity or unevenness represents the main disturbing source for either the passenger or vehicle structure itself. Roads are commonly represented by a Power Spectral Density (PSD) of road profiles. Based on the PSD of roads ISO 8086 [24] classified roads as A, B,...H which is shown in Table 4.1 and the PSD of the road profile is given by Equation 4.1.

$$G_r(n) = G_r(n_o)\left(\frac{n}{n_o}\right)^{-w} \tag{4.1}$$

Where;

$G_r(n_o)$ is road roughness coefficient $(m^3/cycle)$

n is spatial cyclic frequency

$n_o = 0.1\text{cycle}/m$ is reference spatial cyclic frequency

$w = -2$ is road waviness level

When a vehicle moves with a constant velocity v on a road of $G_r(n_o)$, the differential equation of the road excitation can be expressed as in Equation 4.2 [25].

$$\dot{y}_o(t) + 2\pi n_o v y_o(t) = \sqrt{G_r(n_o)\, v}\, w(t) \tag{4.2}$$

Where;

$w(t)$ is white noise signal with PSD of unity

Table 4.2: Road degree of roughness as a function of angular spacial frequency

Road Class	Degree of roughness		
	Lower limit	Geometric mean	Upper limit
	Angular spatial frequency units, Ω		
	$G_r\,(\Omega_o) \times 10^{-6} m^3$		
A	-	1	2
B	2	4	8
C	8	16	32
D	32	64	128
E	128	256	512
F	512	1,024	2,048
G	2,048	4,094	8,192
H	8,192	16,384	-

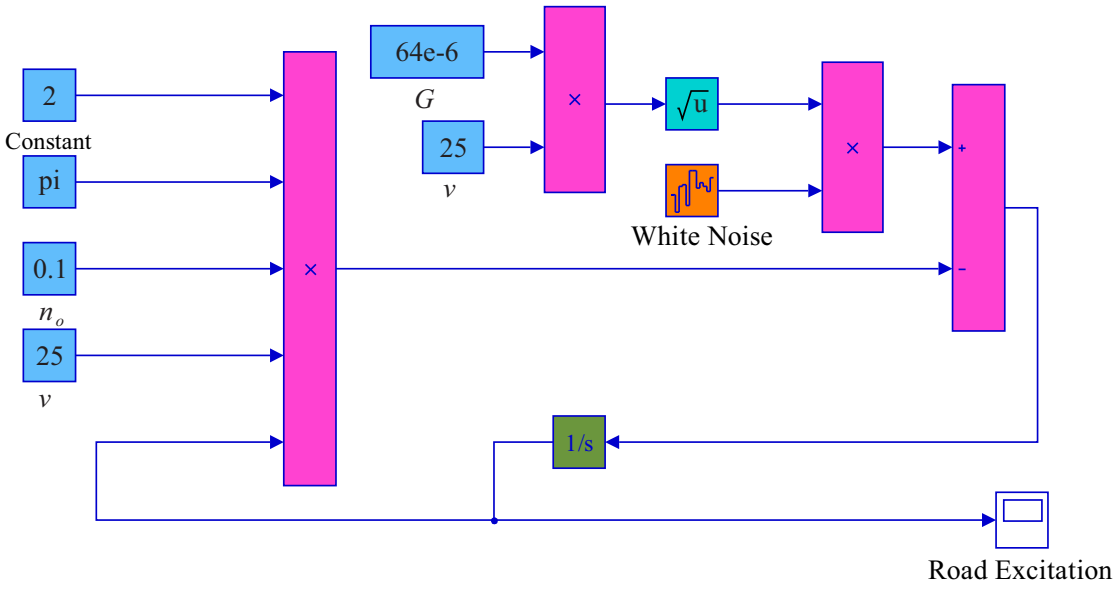

Figure 4.1: Simulink model of class-B Road

For the purpose of analysis, a vehicle moving on an average road of class-B with a geometric mean road roughness coefficient of $64 \times 10^{-6} m^3/cycle$ is used. The vehicle is moving with a constant speed of $90 km/h$.

The road is modelled in Simulink as shown in Figure 4.1 and its road excitation versus time is given in Figure 4.2.

4.3 Optimization Variables

The performance of a suspension system mainly depends on damping coefficient of the suspension system (C), spring stiffness of the suspension system (K_c) and stiffness of

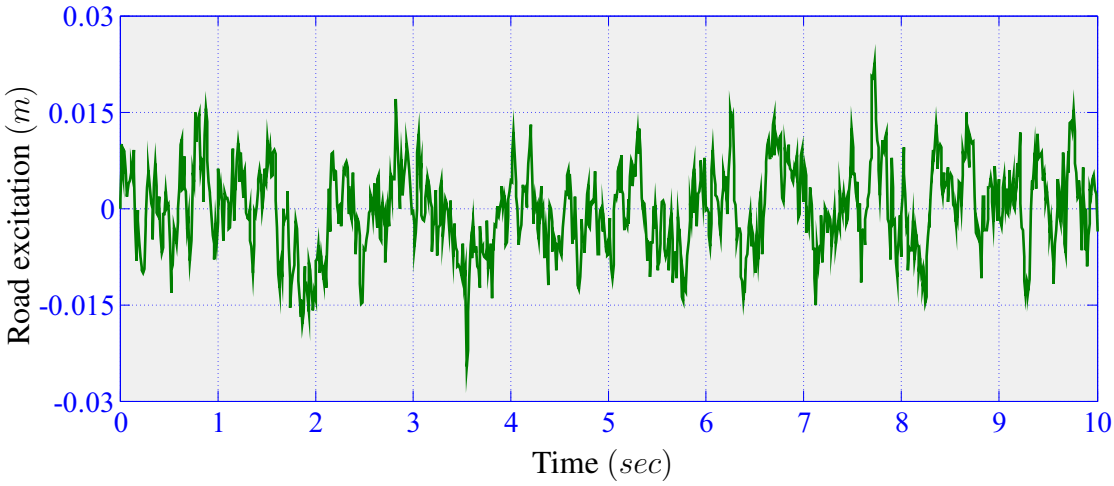

Figure 4.2: Road excitation of class-B Road

the tyre (K_t) of the vehicle itself. For CSS system the optimum value of these three variables have to be determined for better RC and RH.

In ASS system since the spring stiffness (K_a) of the suspension system depends on initial pressure (P_o), volume (V_o) and cross-sectional area (A) of the air cylinder, the optimum value of these variables in addition to damping coefficient (C) and tyre stiffness (K_t) have to be determined.

4.4 Objective Functions

As it is intended to compromise between two conflicting requirements a multi-objective GA optimization technique is employed to determine the best configuration of vehicle parameters. Determining the objective function containing vehicle parameters is the basic task of the optimization process. According to ISO 2631 [26], RC is related to RMS of sprung mass acceleration (a_{RMS}) which is given by Equation 4.3.

$$a_{RMS} = \left\{ \frac{1}{t} \int_0^t \left[\ddot{y}_s \left(t \right) \right]^2 dt \right\}^{1/2} \tag{4.3}$$

Where;

t is the time taken by the vehicle for the motion

Lower value of a_{RMS} corresponds to higher RC and vice versa. Again, RH is related to

RMS of tyre deflection (td_{RMS}) which is given by Equation 4.4.

$$td_{RMS} = \left\{ \frac{1}{t} \int_0^t \left[y_u(t) - y_o(t) \right]^2 dt \right\}^{1/2} \tag{4.4}$$

Where;

t is the time taken by the vehicle for the motion

Lower value of td_{RMS} corresponds to higher RH and vice versa.

Since, both a_{RMS} and td_{RMS} varies with time it is impossible to optimize the vehicle parameters and time simultaneously. Thus, for the purpose of optimization a different equation of a_{RMS} and td_{RMS} that doesn't involve time will be needed.

4.4.1 Objective Functions of CSS system

The objective of employing optimization is achieving better RC and RH by obtaining the optimum configuration of vehicle parameters. This can be done by minimizing a_{RMS} and td_{RMS} simultaneously using multi-objective optimization. The objective functions for CSS system include K_c, K_t and C. Thus they will be in the form of

$$\begin{cases} a_{RMS} = f(K_c, K_t, C) \\ td_{RMS} = f(K_c, K_t, C) \end{cases} \tag{4.5}$$

According to [23, 27], the objective functions of CSS system that doesn't involve time are given by Equation 4.6.

$$\begin{cases} a_{RMS} = \left\{ \pi G v \left[\frac{K_t C}{2 {m_s}^{3/2} {K_c}^{1/2}} + \frac{(m_u + m_s) {K_c}^2}{2 C {m_s}^2} \right] \right\}^{1/2} \\ td_{RMS} = \left\{ \pi G v \left[\frac{{K_t}^2 m_u}{2C(m_u + m_s)^2} + \frac{(m_u + m_s) {K_c}^2}{2 C {m_s}^2} - \frac{K_t K_c m_u}{C m_s (m_u + m_s)} + \frac{C K_c}{2 m_u m_s} \right] \right\}^{1/2} \end{cases} \tag{4.6}$$

Where;

G is given by Equation 4.7 as

$$G = {\Omega_o}^2 G_r(\Omega_o) \left(\frac{\Omega}{\Omega_o} \right)^{-w} \tag{4.7}$$

Where;

$G_r(\Omega_o)$ is road roughness coefficient $(m_3/cycle)$

Ω is spatial angular frequency

$\Omega_o = 1\ rad/m$ is reference spatial angular frequency

$w = -2$ is road waviness level

In Table 4.2 for class-B road, $G = 4 \times 10^{-6} m^3/cycle$

The objective function is subjected to an inequality constraint of RMS of suspension working space sw_{RMS} which is given by Equation 4.8 [23, 27].

$$sw_{RMS} = \left\{ \pi G v \left[\frac{(m_u + m_s)\,(m_s K_c)^{1/2}}{2C m_s} \right] \right\}^{1/2} \leq 0.05 \tag{4.8}$$

4.4.2 Objective Functions of ASS system

The objective functions for ASS system include P_o, A, V_o, K_t and C or P_o, r, h_o, K_t and C. Thus they will be in the form of

$$\begin{cases} a_{RMS} = f\,(P_o, A, V_o, K_t, C) = f\,(P_o, r, h_o, K_t, C) \\ td_{RMS} = f\,(P_o, A, V_o, K_t, C) = f\,(P_o, r, h_o, K_t, C) \end{cases} \tag{4.9}$$

Substituting $K_c = K_a$ in Equation 4.6 the objective functions for ASS system will become

$$\begin{cases} a_{RMS} = \left\{ \pi G v \left[\frac{K_t C}{2 {m_s}^{3/2} {K_a}^{1/2}} + \frac{(m_u + m_s) {K_a}^2}{2C {m_s}^2} \right] \right\}^{1/2} \\ td_{RMS} = \left\{ \pi G v \left[\frac{{K_t}^2 m_u}{2C(m_u + m_s)^2} + \frac{(m_u + m_s) {K_a}^2}{2C {m_s}^2} - \frac{K_t K_a m_u}{C m_s (m_u + m_s)} + \frac{C K_a}{2 m_u m_s} \right] \right\}^{1/2} \end{cases} \tag{4.10}$$

Then, substituting $K_a = \frac{\gamma A^2 P_o}{V_o} = \frac{\gamma \pi P_o r^2}{h_o}$ in Equation 4.10,

$$\begin{cases} a_{RMS} = \left\{ \pi G v \left[\frac{{h_o}^{1/2} K_t C}{2 {m_s}^{3/2} (\gamma\pi)^{1/2} {P_o}^{1/2} r} + \frac{(m_u + m_s)(\gamma\pi)^2 {P_o}^2 r^4}{2 {m_s}^2 {h_o}^2 C} \right] \right\}^{1/2} \\ td_{RMS} = \left\{ \pi G v \left[\frac{m_u {K_t}^2}{2(m_u + m_s)^2 C} + \frac{(m_u + m_s)(\gamma\pi)^2 {P_o}^2 r^4}{2 {m_s}^2 {h_o}^2 C} - \frac{m_u \gamma\pi P_o r^2 K_t}{m_s (m_u + m_s) h_o C} + \frac{\gamma\pi P_o r^2 C}{2 m_u m_s h_o} \right] \right\}^{1/2} \end{cases} \tag{4.11}$$

The inequality constraint is obtained by replacing $K_c = K_a = \frac{\gamma\pi P_o r^2}{h_o}$ into Equation 4.8.

$$sw_{RMS} = \left\{ \pi G v \left[\frac{(m_u + m_s)\,(m_s \gamma\pi P_o)^{1/2} r}{2C m_s {h_o}^{1/2}} \right] \right\}^{1/2} \leq 0.05 \tag{4.12}$$

4.5 Optimization Process in MATLAB

MATLAB provides a built-in optimization tool/module which includes Genetic Algorithm. The optimization module of MATLAB has an interface to choose among the different optimization techniques. The default optimization tool window of MATLAB is provided in Appendix-I.

Since it is intended to compromise between two conflicting objectives i.e., a_{RMS} and td_{RMS}, a multi-objective Genetic Algorithm is needed. This is done by choosing "gamultiobj-Multiobjective optimization using Genetic Algorithm" in the optimization module solver of MATLAB.

4.5.1 Optimization process of CSS system

A MATLAB script file which is a user defined function containing the objective functions of CSS system is fed to MATLAB optimization module as a fitness function. This user defined function is provided in Appendix-III. The objective functions of CSS system have three variables namely spring stiffness (K_c), tyre stiffness (K_t) and damping coefficient (C). So the number of variables that the GA optimization module took is 3. All other settings of the optimization module uses the default settings except the "Multi-objective problem settings (Pareto front population fraction)" which is 0.8. The automatically generated code for CSS system optimization process is given in Appendix-II. Running the optimization module gives a "Pareto front" which is the graph of a_{RMS} versus td_{RMS} at each generation, Figure 4.3.

Since GA is a stochastic optimization technique it gives different optimum values for different running of the optimization process. Even though the numerical values are different there is no much difference between them. Optimum found at 7 generations and the values are given in Table 4.3. A single objective GA for RC is also conducted, but it results in an increase of RH.

The optimized model of CSS system is simulated in Simulink and the response of sprung mass acceleration is given in Figure 4.4 and that of tyre deflection is shown in figure 4.5. In both figure the responses are irregular because of the irregularity of the road condition.

Table 4.3: Optimized value of CSS system

Parameters	**Units**	**Original value**	**Optimized Value (Multi-objective GA)**	**Optimized Value (Single objective GA for RC)**
K_c	*N/m*	20,000	10,647	10,000
K_t	*N/m*	200,000	152,250	150,000
C	*N.s/m*	1,500	2,274.5	1,193.9
a_{RMS}	m/s^2	1.335	1.292	0.9825
td_{RMS}	*m*	0.004970	0.004842	0.005599

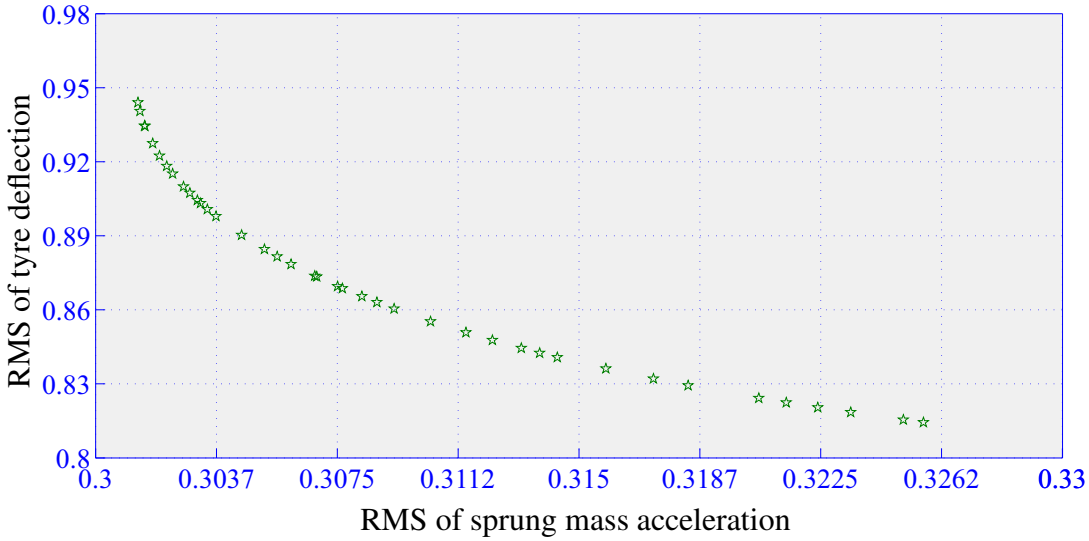

Figure 4.3: Pareto front for multi-objective optimization of CSS system

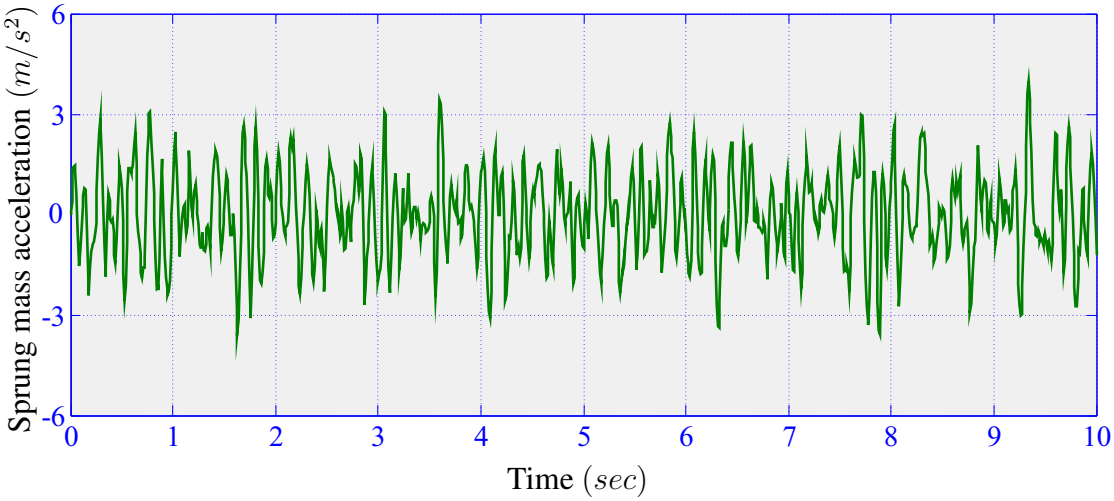

Figure 4.4: Sprung mass acceleration of optimized CSS system

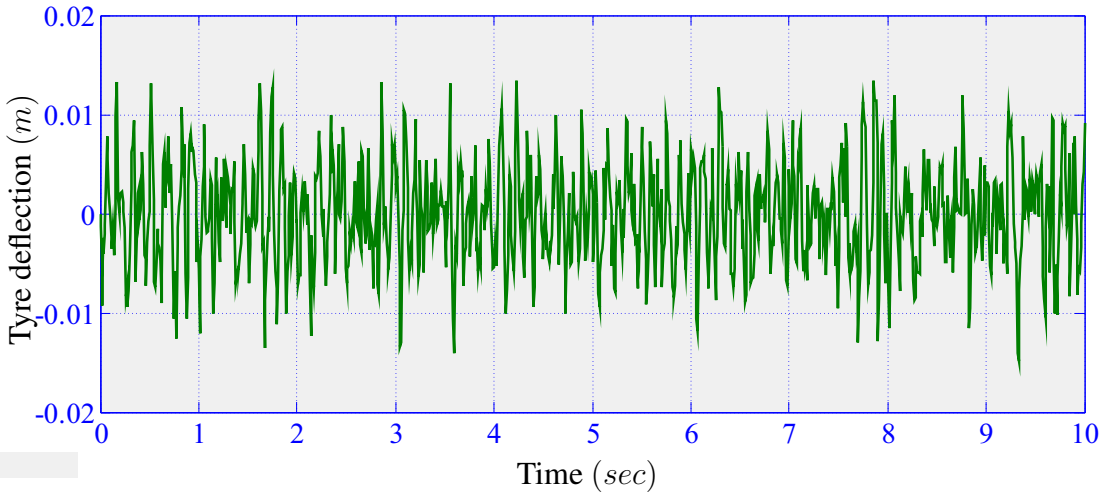

Figure 4.5: Tyre deflection of optimized CSS system

Table 4.4: Optimized value of ASS system

Parameters	**Units**	**Original value**	**Optimized Value (Multi-objective GA)**	**Optimized Value (Single objective GA for RC)**
P_o	*Pa*	600,000	533,610	504,740
r	*m*	0.04675	0.043	0.0364
h_o	*m*	0.2884	0.3496	0.3498
K_t	*N/m*	200,000	152,910	150,001.3
C	*N.s/m*	1,500	2,169.4	1109.5
a_{RMS}	m/s^2	1.335	1.275	0.946
td_{RMS}	*m*	0.004970	0.004834	0.005789

4.5.2 Optimization process of ASS system

A MATLAB script file which is a user defined function containing the objective functions of ASS system is fed to MATLAB optimization module as a fitness function. This user defined function is provided in Appendix-V. The objective functions of ASS system have five variables namely initial pressure (P_o), air cylinder radius (r), air cylinder height (h_o), tyre stiffness (K_t) and damping coefficient (C). So the number of variables that the GA optimization module took is 5. All other settings of the optimization module uses the default settings except the "Multi-objective problem settings (Pareto front population fraction)" which is 0.8. The automatically generated code for ASS system optimization process is given in Appendix-IV. Running the optimization module gives a "Pareto front" which is the graph of a_{RMS} versus td_{RMS} at each generation, Figure 4.6. Optimum found at 27 generations and the values are given in Table 4.4.

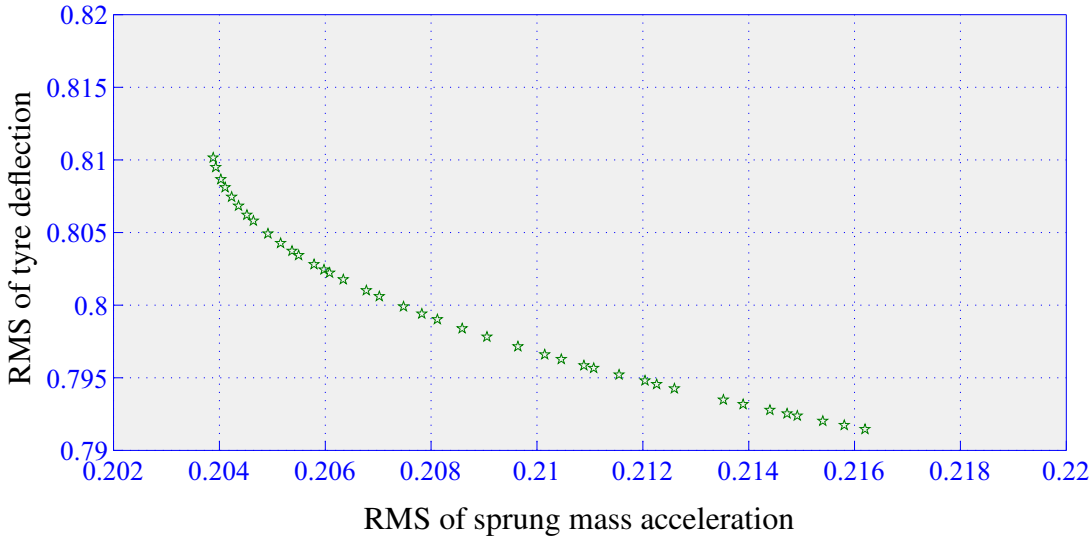

Figure 4.6: Pareto front for multi-objective optimization of ASS system

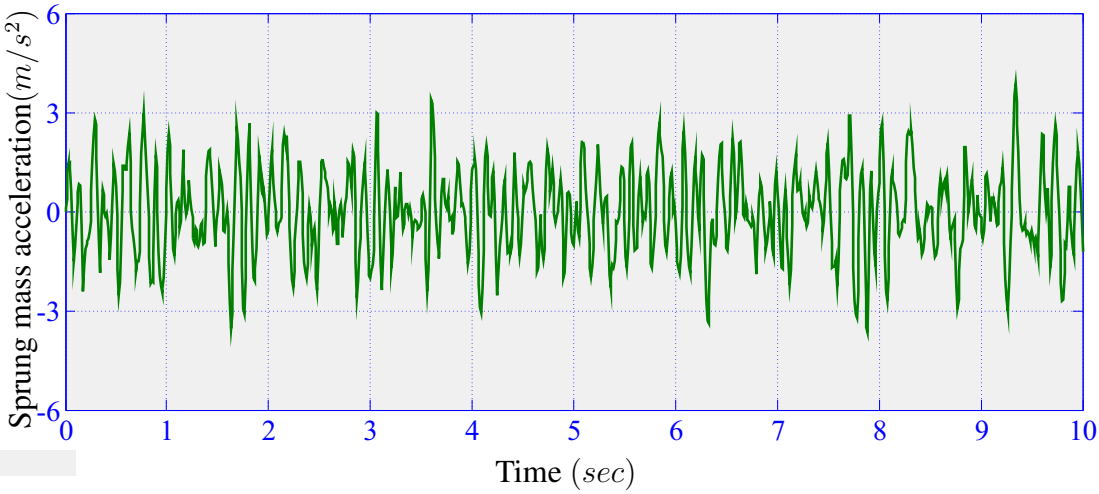

Figure 4.7: Sprung mass acceleration of optimized ASS system

The optimized model of ASS system is also simulated in Simulink and the response of sprung mass acceleration is given in Figure 4.7 and that of tyre deflection is shown in figure 4.8. In both figure the responses are irregular because of the irregularity of the road condition.

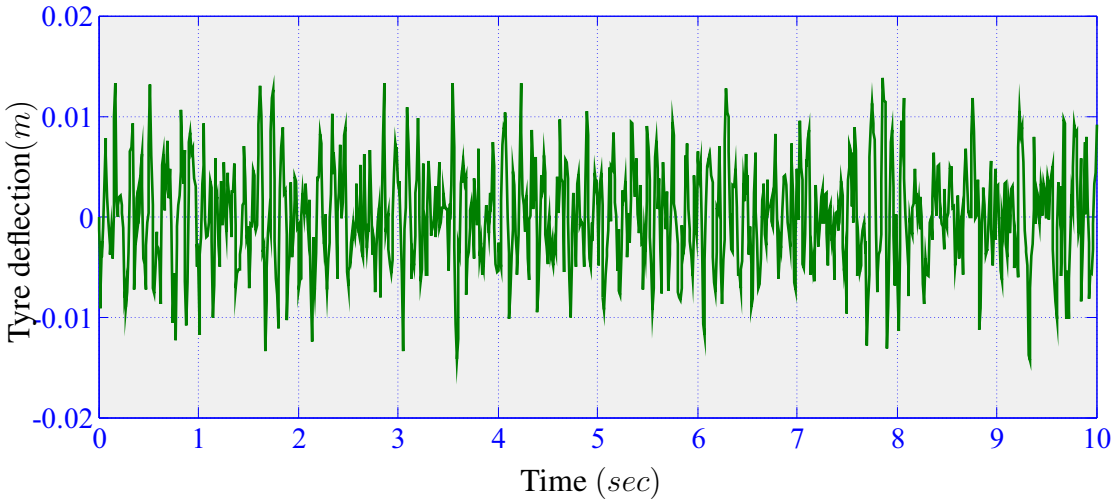

Figure 4.8: Tyre deflection of optimized ASS system

CHAPTER 5

FUZZY LOGIC CONTROLLER

In this chapter, Fuzzy Logic Controller is developed for the optimized models of CSS and ASS system. The developed Fuzzy Logic controller is a modern type rather than classical which uses error signal as on of the control input. Then the controller is integrated to both models and simulated in Simulink to show the responses.

5.1 Active Suspension System

Vehicles with passive suspension system can't provide efficient RC and RH simultaneously. This is because as RC increases RH decreases. There is an optimum point to keep the RC and RH in balance. This point is obtained by applying appropriate spring and damper coefficient through optimization. Even though optimized passive model is used it is not good enough to provide the required RC and RH for the modern luxurious vehicles.

Today active suspension systems are being used to achieve better RC and RH at the same time. This is obtained by integrating a double acting cylinders or solenoids (actuators) between sprung mass and unsprung mass for each wheel. The cylinders or actuators provide a controlled actuator force to considerably improve the ride quality. In active suspension system, the mathematical model contains an actuator force in addition to passive models.

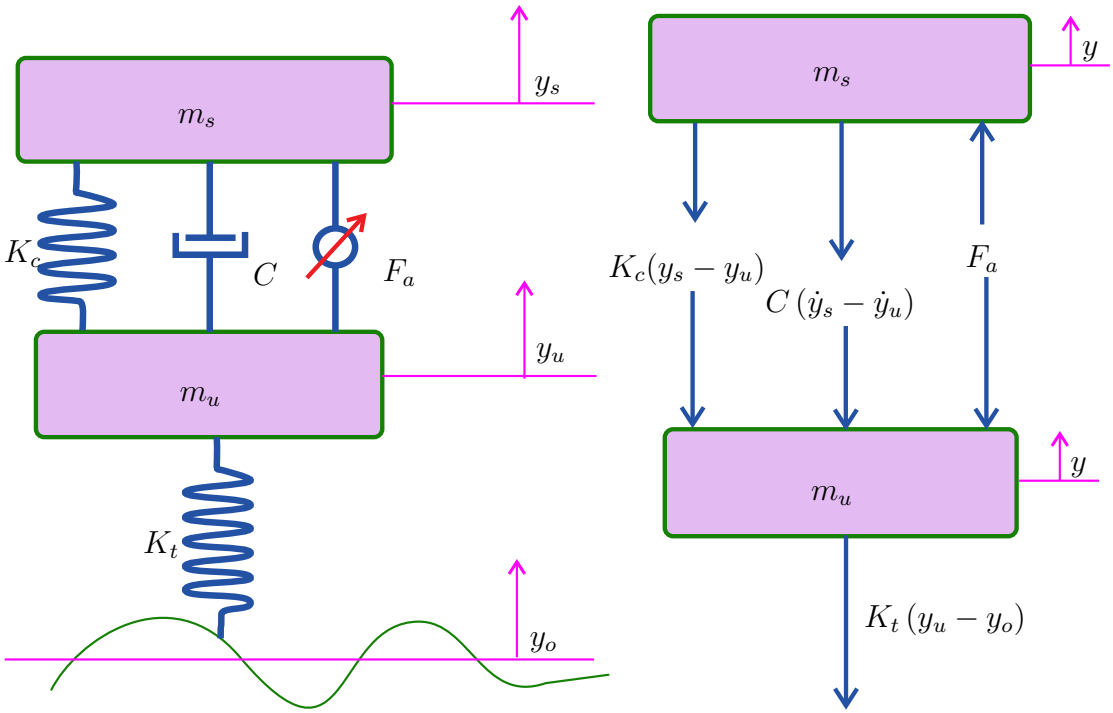

Figure 5.1: Dynamic model of Quarter Car Active CSS system

5.1.1 Active CSS system Mathematical Model

Figure 5.1 gives an Active CSS model which includes an actuating force. Applying Newton's second law to the free body diagram of sprung mass, in Figure 5.1,

$$\sum F_y = m_s \ddot{y}_s$$
$$m_s \ddot{y}_s + C\,(\dot{y}_s - \dot{y}_u) + K_c\,(y_s - y_u) - F_a = 0 \tag{5.1}$$

Applying Newton's second law to the free body diagram of unsprung mass, in Figure 5.1,

$$\sum F_y = m_u \ddot{y}_u$$
$$m_u \ddot{y}_u - C\,(\dot{y}_s - \dot{y}_u) - K_c\,(y_s - y_u) + K_t\,(y_u - y_o) + F_a = 0 \tag{5.2}$$

5.1.2 Active CSS system Simulink Model

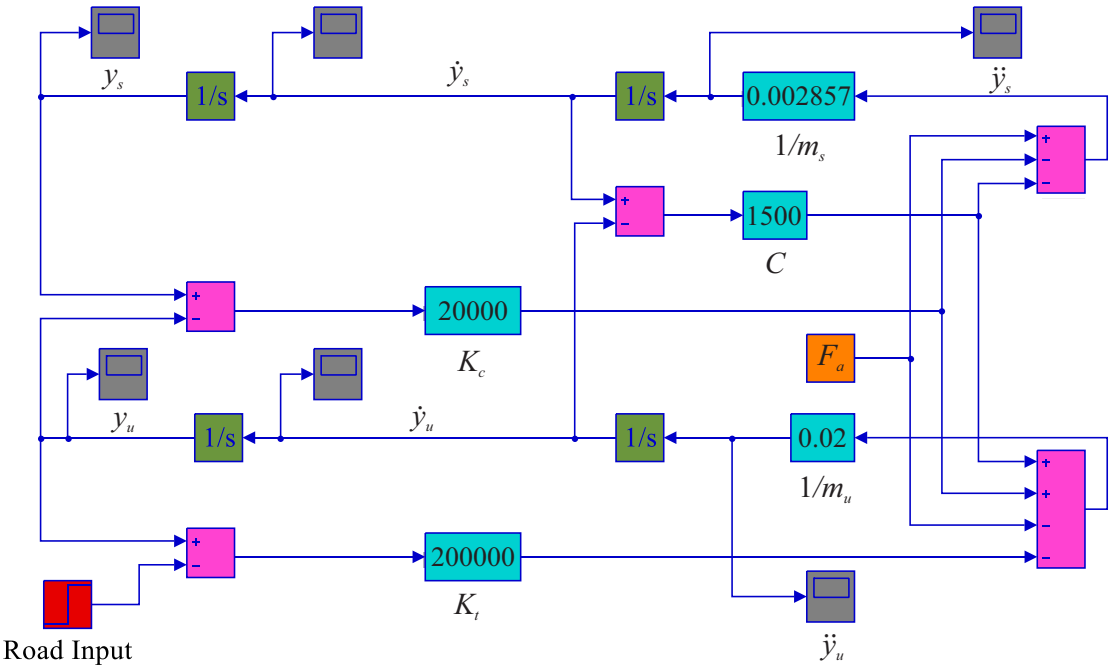

Figure 5.2: Simulink Model of Quarter Car Active CSS system

5.1.3 Active ASS system Mathematical Model

Applying Newton's second low to the free body diagram of sprung mass, in Figure 5.3,

$$\sum F_y = m_s \ddot{y}_s$$

$$m_s \ddot{y}_s + C\left(\dot{y}_s - \dot{y}_u\right) + AP_o\left\{\left[\frac{h_o}{h_o - (y_s - y_u)}\right]^{\gamma} - 1\right\} - F_a = 0 \tag{5.3}$$

Applying Newton's second low to the free body diagram of unsprung mass, in Figure 5.3,

$$\sum F_y = m_u \ddot{y}_u$$

$$m_u \ddot{y}_u - C\left(\dot{y}_s - \dot{y}_u\right) - AP_o\left\{\left[\frac{h_o}{h_o - (y_s - y_u)}\right]^{\gamma} - 1\right\} + K_t\left(y_u - y_o\right) + F_a = 0 \tag{5.4}$$

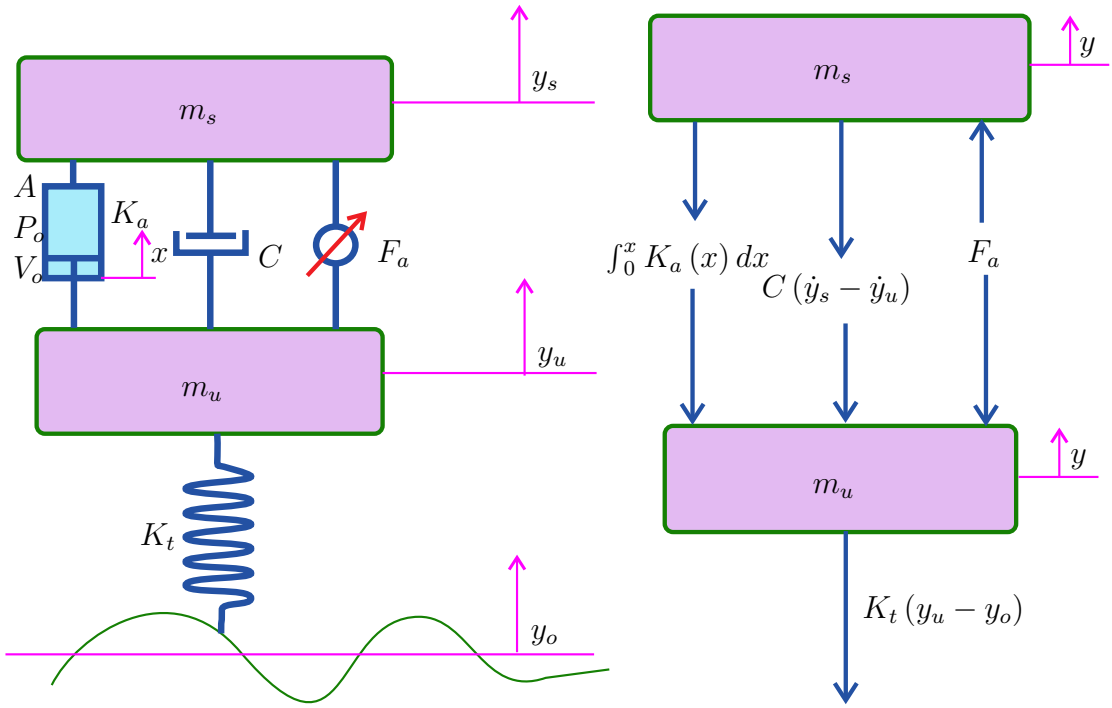

Figure 5.3: Dynamic model of Quarter Car Active ASS system

5.1.4 Active ASS system Simulink Model

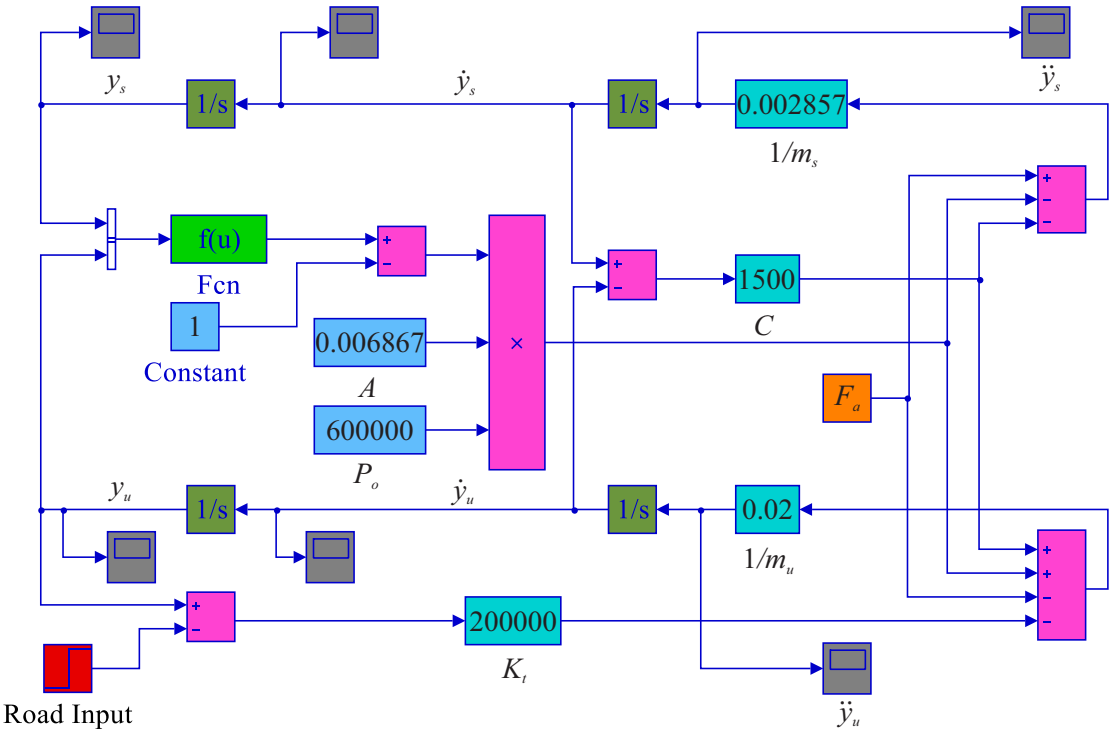

Figure 5.4: Simulink Model of Quarter car Active ASS system

Vehicle suspension system parameters are continually changing and become non-linear as the vehicle rides on different road conditions. The beauty of FLC is that, it doesn't depend on the accuracy of the mathematical model and it can easily capture the non-linearities [28].

5.2 Introduction to Fuzzy Logic Controller

Fuzzy logic is derived from fuzzy set theory dealing with reasoning which is approximate rather than precisely deduced from classical predicate logic. It is a super set of conventional (Boolean) logic that has been extended to handle the concept of partial truth central notion of fuzzy systems is that truth values (in fuzzy logic) or membership values (in fuzzy sets) are indicated by a value on the range [0.0, 1.0], with 0.0 representing absolute Falseness and 1.0 representing absolute Truth. It deals with real world vagueness. Member ship function describes the certainty that the element described linguistically belongs to the fuzzy set [29]. The number of necessary fuzzy sets and their ranges are designed based up on the experience gained by the process [28].

The concept of fuzzy logic was first introduced by 1965 by a computer scientist Zadeh, a professor at the University of California. Fuzzy logic allows the program to deal with natural, linguistic sets of states, as such as very fast, fast, slow, etc. fuzzy-logic provides a simple way to arrive at a define conclusion based upon ambiguous, imprecise, noisy or missing input information. Fuzzy logic incorporates a simple, rule-based IF X AND Y THEN Z approach to a solving control problem rather than trying to model a system mathematically. The fuzzy rule depends on an operators experience rather than their technical understanding of the system [30].

The basic ideal of fuzzy logic control is to include the knowledge of a human work in the design of a controller in controlling a procedure whose input-output relationship is defined by gathering of fuzzy control rules containing linguistic variables. The design technique of Fuzzy Logic Controller (FLC) is based upon knowledge derived from imprecise heuristic knowledge of experienced operator, and it doesn't require precise knowledge of the system model [30].

A FLC converts a linguistic control strategy into an automatic controller capable of

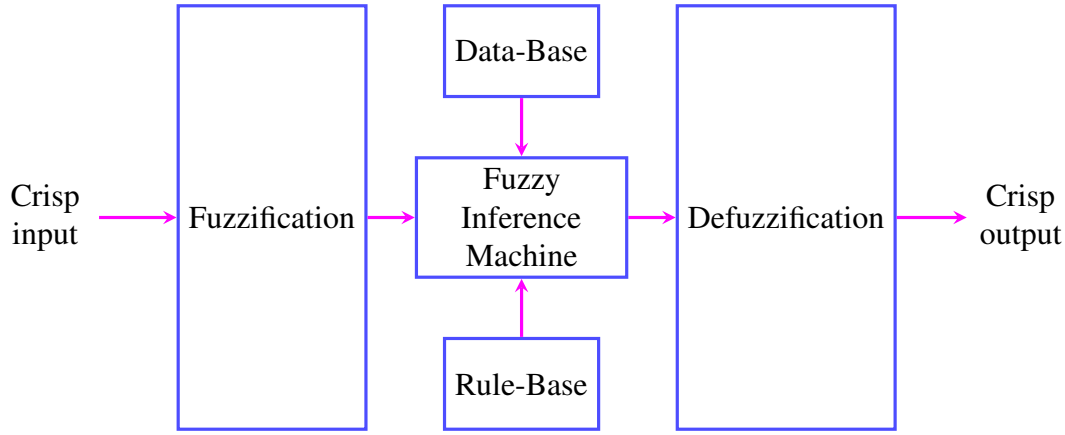

Figure 5.5: Fuzzy Logic Controller Architecture

managing the non-linearities and uncertainties of the active suspension system.

The development of FLC consists of Fuzzification, Decision making logic (fuzzy inference machine) and Defuzzification [28]. This is shown in Figure 5.5 below. Fuzzification transforms real (crisp) values in to linguistic (fuzzy) values that are later manipulated by the fuzzy rule-base and decision making process [31, 32]. The fuzzy rule is in the form of linguistic variables using the fuzzy condition statement. It is composed of antecedent (if-clause) and consequent (then-clause) [27]. The fuzzy inference machine processes the input fuzzy value and computes the controller output fuzzy value in cope with rule-base and data-base [32, 33]. Defuzzification transforms linguistic (fuzzy) values into real (crisp) values that are fed into the controlled system [32, 33].

5.3 Development of FLC in MATLAB

The development of FLC begins by identifying control inputs and output. FLC is being developed which is different from classical FLC. The difference is in that classical FLC uses error signal as one of the control inputs. There are three control inputs namely, tyre deflection $(y_u - y_o)$, suspension travel/deflection $(y_s - y_u)$ and deflection velocity $(\dot{y}_s - \dot{y}_u)$. The control output is only the actuating force (F_a). These control inputs and outputs are divided into fuzzy sets which are different from ordinary set by having degree of membership. Limiting the boundaries of fuzzy sets is a crucial task in FLC development. Figure 5.6 through Figure 5.9 show the membership functions for control inputs and control output.

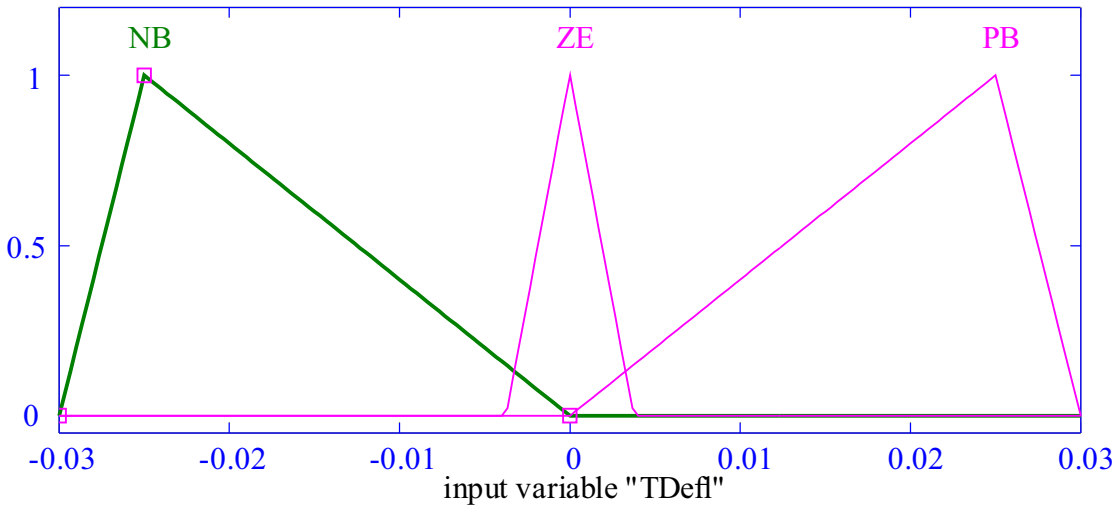

Figure 5.6: Membership function of Tyre Deflection

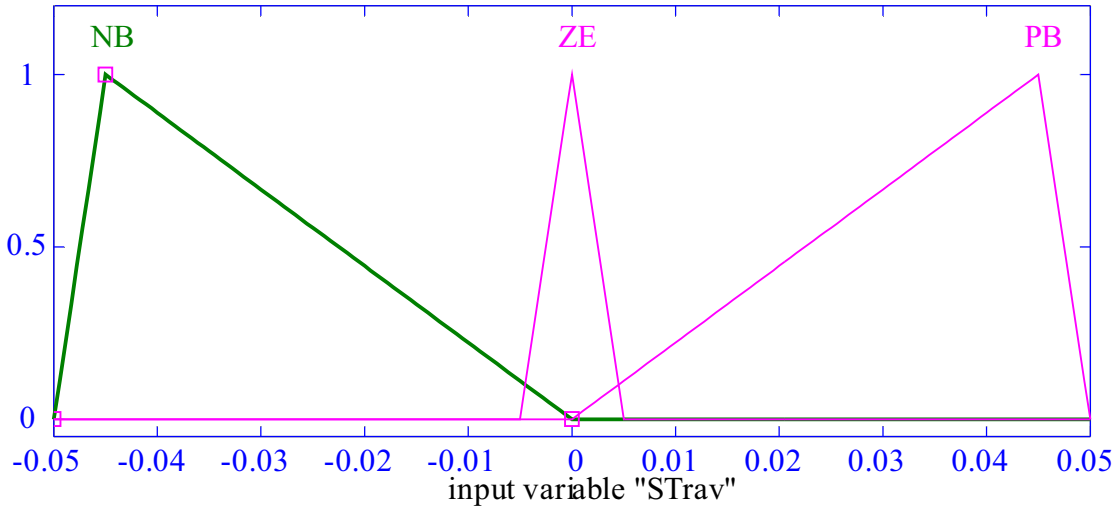

Figure 5.7: Membership function of Suspension Travel

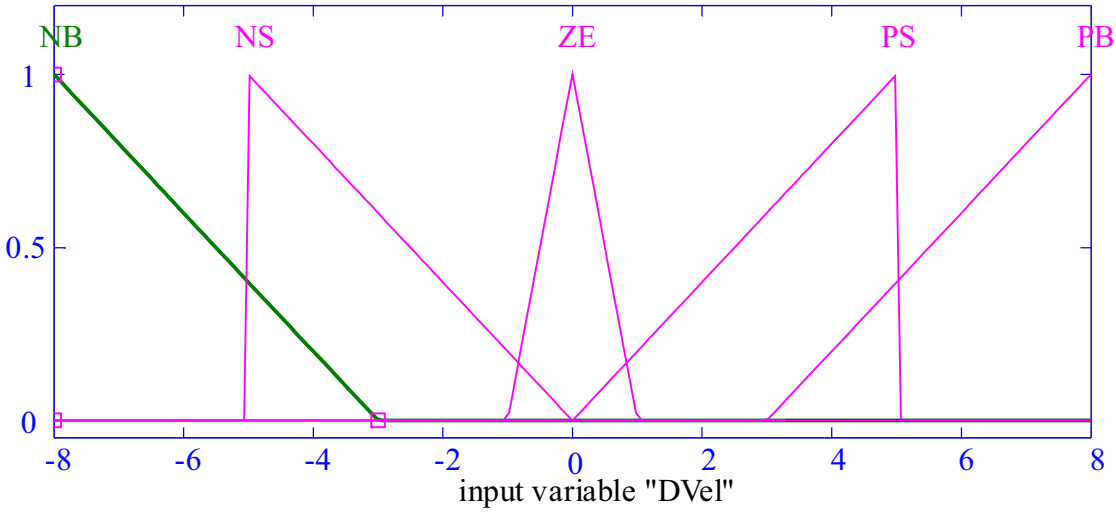

Figure 5.8: Membership function of Deflection Velocity

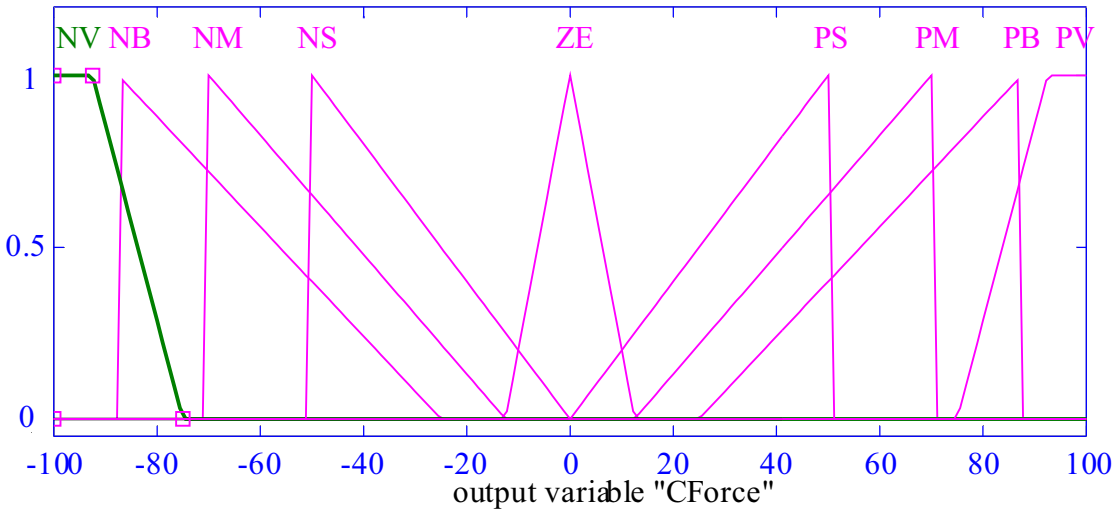

Figure 5.9: Membership function of Controlling Force

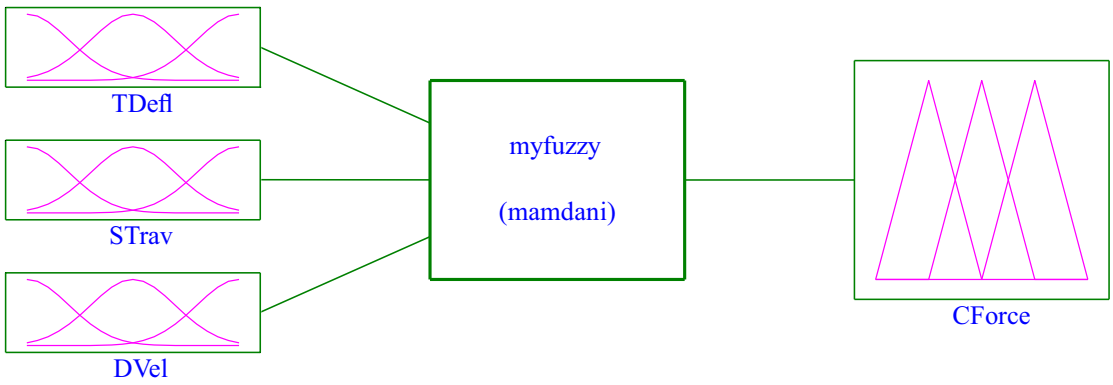

Figure 5.10: Input-Output configuration of FLC

The control output and inputs should have given an appropriate scaling factor in order to incorporate the various ranges of output and inputs. This is because the fuzzy variables are in a range of [-1, 1] and it should account for all the necessary range of output and inputs.

The fuzzy logic variables are combined to give the FLC input-output configuration shown in Figure 5.10. The different fuzzy sets are combined by if-then statement to give the fuzzy rule-base which is the brain of FLC. The if-then statement is like,

$$\text{If } (y_u - y_o = A) \text{ and } (y_s - y_u = B) \text{and} (\dot{y}_s - \dot{y}_u = C), \text{ then } (F_a = E).$$

Where *A*, *B*, *C* and *D* are the membership functions for tyre deflection, suspension travel, deflection velocity, and actuating force respectively.

A total of 45 fuzzy rules are formulated to control quarter car suspension system. All the rules are given in Table 5.1.

Table 5.1: FLC Rules

№	$y_u - y_o$	$y_s - y_u$	$\dot{y}_s - \dot{y}_u$	F_a	№	$y_u - y_o$	$y_s - y_u$	$\dot{y}_s - \dot{y}_u$	F_a
1	NB	NB	NB	PV	24	ZE	ZE	PS	NS
2	NB	NB	NS	PB	25	ZE	ZE	PB	NB
3	NB	NB	ZE	PS	26	ZE	PB	NB	PM
4	NB	NB	PS	ZE	27	ZE	PB	NS	PS
5	NB	NB	PB	NM	28	ZE	PB	ZE	NS
6	NB	ZE	NB	PB	29	ZE	PB	PS	NM
7	NB	ZE	NS	PM	30	ZE	PB	PB	NB
8	NB	ZE	ZE	PS	31	PB	NB	NB	PB
9	NB	ZE	PS	NS	32	PB	NB	NS	PM
10	NB	ZE	PB	NM	33	PB	NB	ZE	ZE
11	NB	PB	NB	PB	34	PB	NB	PS	NS
12	NB	PB	NS	PS	35	PB	NB	PB	NB
13	NB	PB	ZE	ZE	36	PB	ZE	NB	PM
14	NB	PB	PS	NS	37	PB	ZE	NS	PS
15	NB	PB	PB	NB	38	PB	ZE	ZE	NS
16	ZE	NB	NB	PB	39	PB	ZE	PS	NM
17	ZE	NB	NS	PM	40	PB	ZE	PB	NB
18	ZE	NB	ZE	PS	41	PB	PB	NB	PM
19	ZE	NB	PS	NS	42	PB	PB	NS	ZE
20	ZE	NB	PB	NM	43	PB	PB	ZE	NS
21	ZE	ZE	NB	PB	44	PB	PB	PS	NB
22	ZE	ZE	NS	PS	45	PB	PB	PB	NV
23	ZE	ZE	ZE	ZE					

5.4 Integration of FLC to the Quarter Car Suspension System in Simulink

The developed FLC is applied to both CSS and ASS system by using appropriate scaling factors to the FLC variables since both systems respond differently.

5.4.1 Integration of FLC to CSS system

The FLC is integrated to the CSS system which then becomes active CSS system, whose Simulink model is shown in Figure 5.11. The scaling factors for tyre deflection, suspension travel, deflection velocity, and actuating force are 0.1, 1, 3 and 0.0002 respectively. The response of active CSS system with FLC on class-B road for sprung mass acceleration and sprung mass displacement is given in Figure 5.13 and Figure 5.14, respectively with much improvement in vehicle performances.

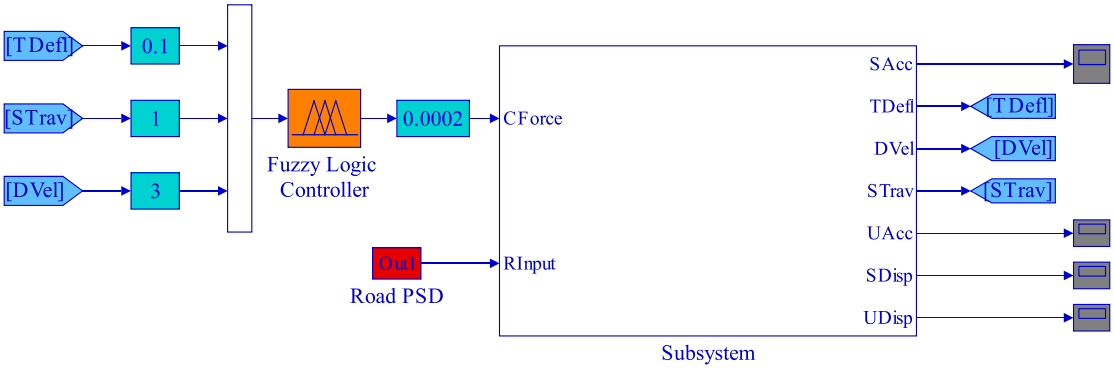

Figure 5.11: Active CSS system with FLC

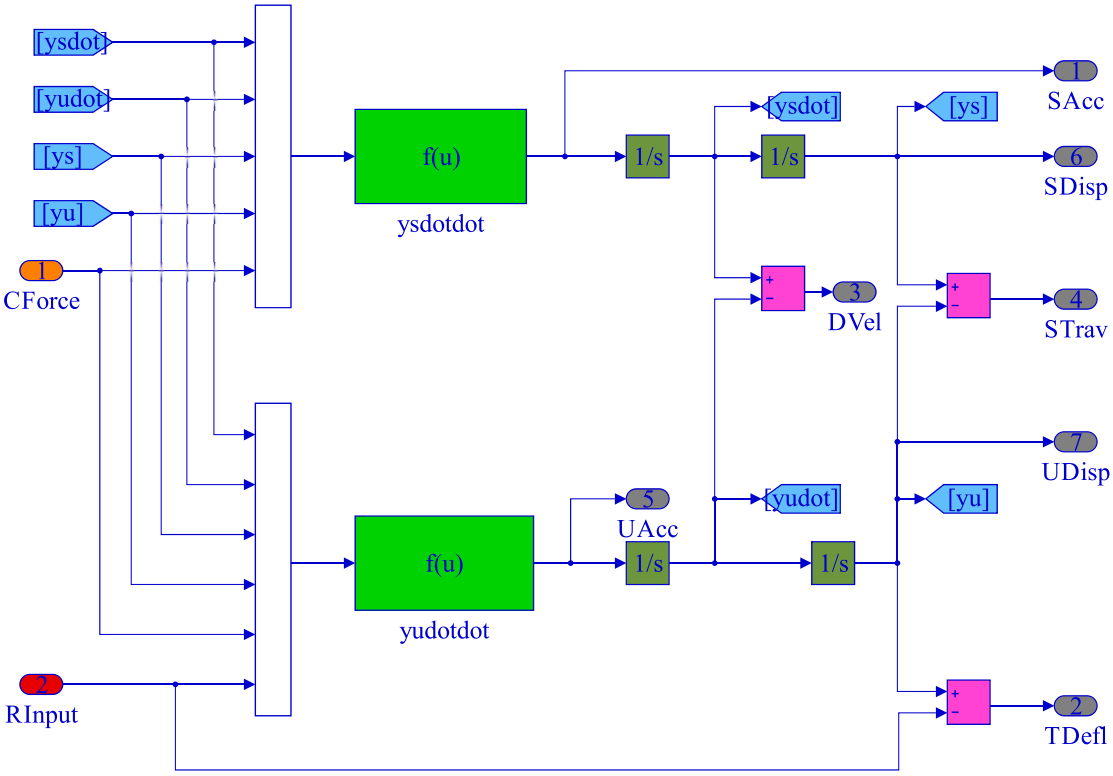

Figure 5.12: The subsystem of Figure 5.11

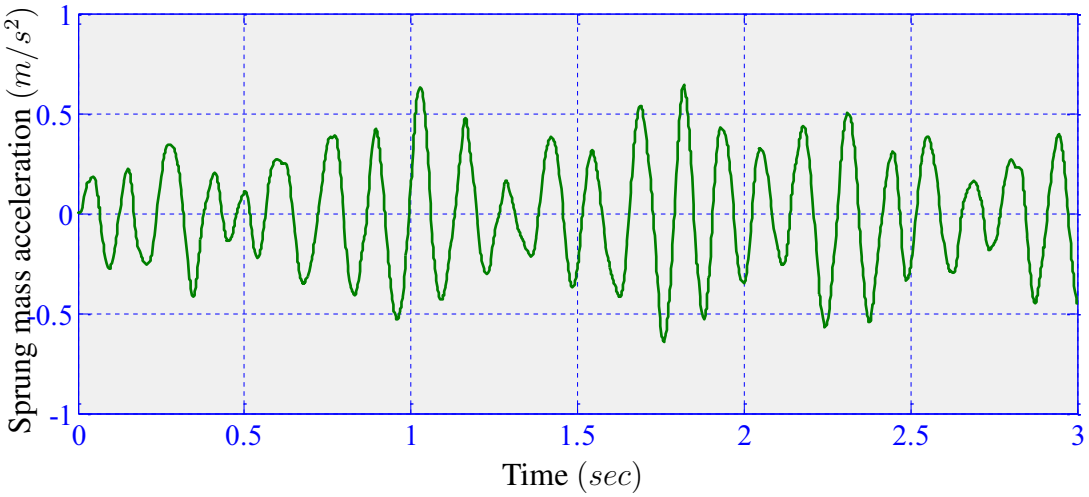

Figure 5.13: Sprung mass acceleration of Active CSS system

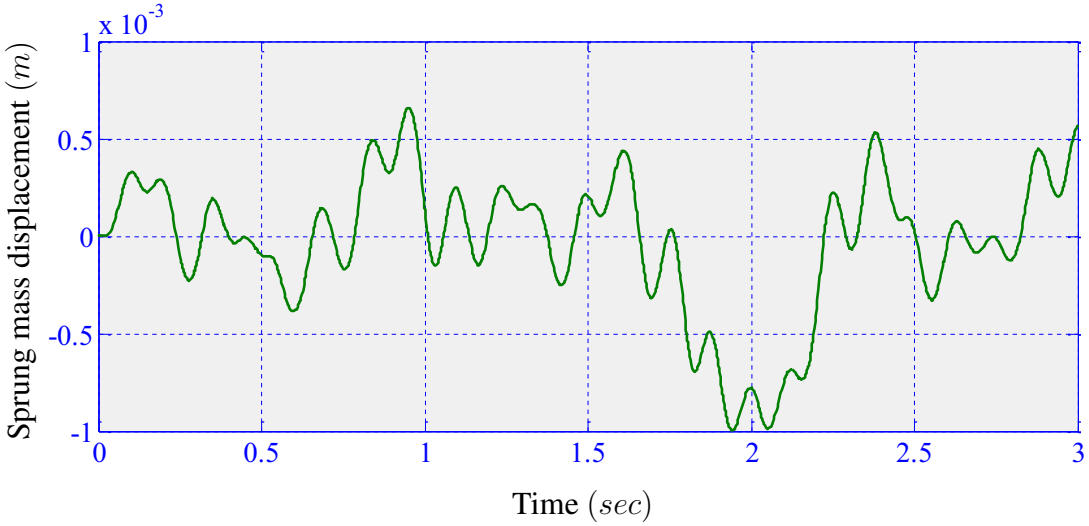

Figure 5.14: Sprung mass displacement of Active CSS system

5.4.2 Integration of FLC to ASS system

The FLC is integrated to the ASS system which then becomes active ASS system, whose Simulink model is shown in Figure 5.17. The scaling factors for tyre deflection, suspension travel, deflection velocity and actuating force are 0.015, 0.02, 1.67 and 0.00045 respectively. The response of active ASS system with FLC on class-B road for sprung mass acceleration and sprung mass displacement is given in Figure 5.17 and Figure 5.18, respectively with much improvement in vehicle performances.

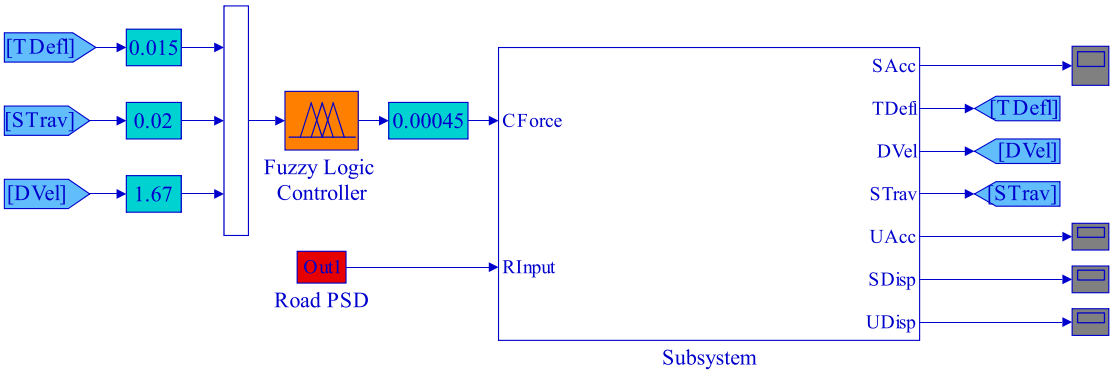

Figure 5.15: Active ASS system with FLC

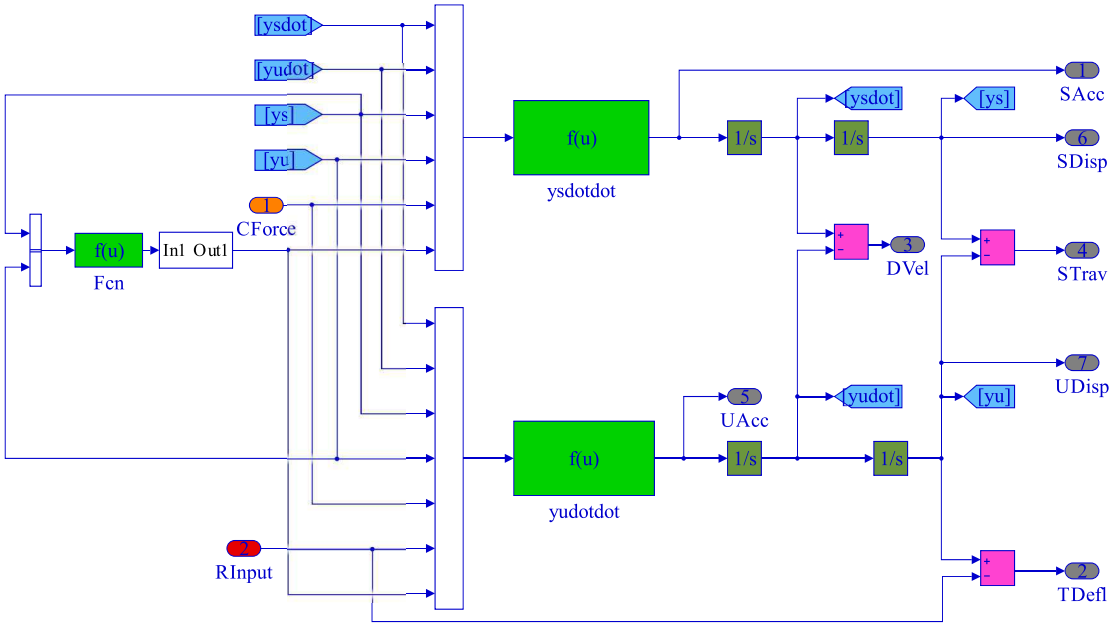

Figure 5.16: The subsystem of Figure5.17

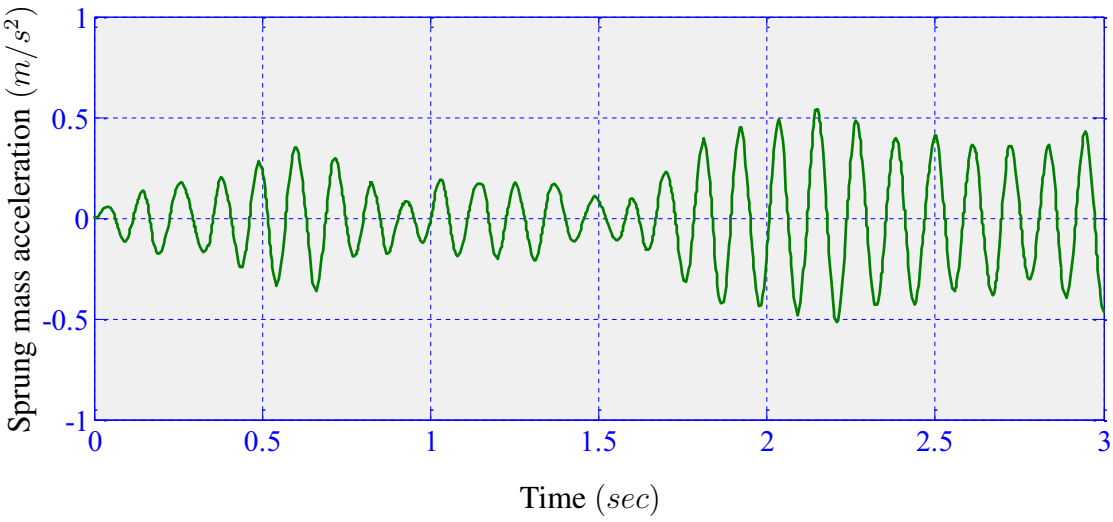

Figure 5.17: Sprung mass acceleration of Active ASS system

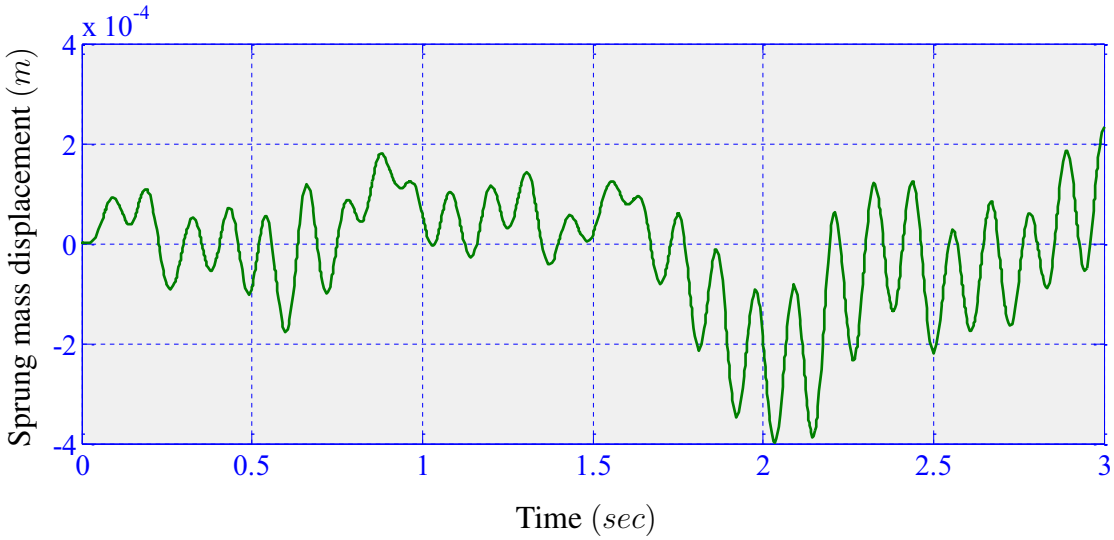

Figure 5.18: Sprung mass displacement of Active ASS system

6 CHAPTER

RESULTS AND DISCUSSION

Smart approach of presenting research result with clear discussion is the heart of a research report. In this chapter, different simulation results of quarter car are presented with their discussion. The different simulations run for different time interval depending on the visibility of the graphs. This does not hurt the simulation result because the road input has a constant varying range. The effect of optimization on CSS and ASS system is separately provided and then compared between the two systems. Sprung mass variation affects RC and RH. This phenomenon is also compared between CSS and ASS system. FLC is employed on both CSS and ASS system. The response of the two systems to FLC is revealed separately and then compared as well.

6.1 Comparing Optimized Passive CSS and ASS system

6.1.1 Comparing Original and Optimized CSS system

To show the effect of optimization on CSS system, a Simulink model of quarter car with original and optimized parameter run together for 10 seconds. One of the simulation results is sprung mass acceleration with its RMS value shown in Figure 6.1. RC is measured in RMS of sprung mass acceleration, with indirect relationship i.e. lower value of RMS of sprung mass acceleration corresponds to good RC and vice versa. From the figure, the RMS value of sprung mass acceleration is decreased from 1.335% to 1.292 m/s^2 by optimization. This change is -3.22%, which results in an increase of RC by 3.22%. The effect of optimization is also observed on RH which is measured by tyre deflection with indirect relationship. Figure 6.2 shows tyre deflection

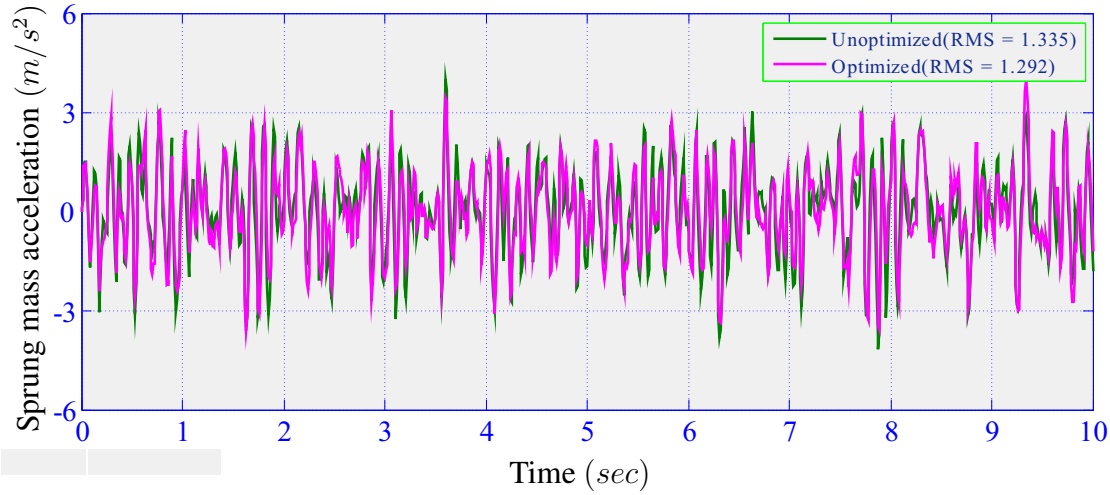

Figure 6.1: Sprung mass acceleration of original and optimized CSS system

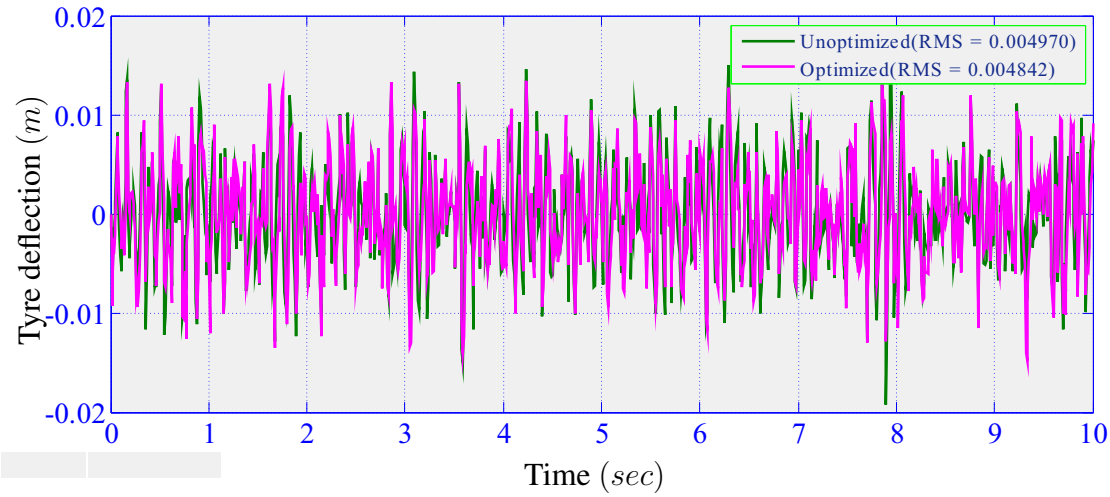

Figure 6.2: Tyre deflection of original and optimized CSS system

with its RMS value for original and optimized CSS system. Optimization also reduces RMS value of tyre deflection by 2.58%. This leads to an improvement of RH by 2.58%. These results are obtained by multi-objective optimization. In the need to improve both RC and RH by multi-objective optimization, the improvements are not such tremendous. In single objective optimization for RC, RMS value of sprung mass acceleration reduced from 1.335 to 0.9825 m/s^2, which implies a RC increase of 26.4%. This reveals an improvement of RC in single objective optimization is more than multi-objective optimization, but it causes a decrease of RH by 12.66%.

6.1.2 Comparing Original and Optimized ASS system

Simulink model of quarter car with original and optimized parameter run together for 10 seconds to demonstrate the influence of optimization on ASS system too. Sprung

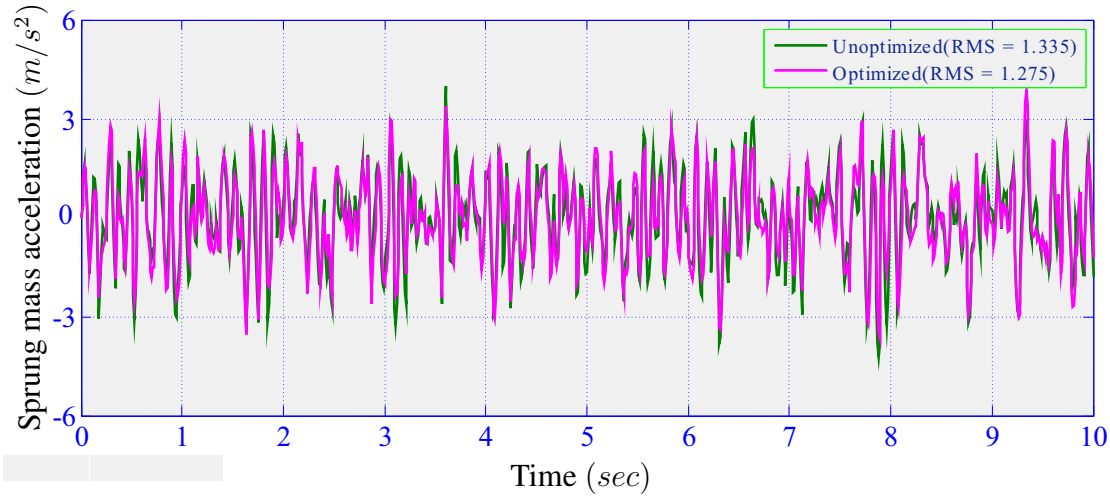

Figure 6.3: Sprung mass acceleration of original and optimized ASS system

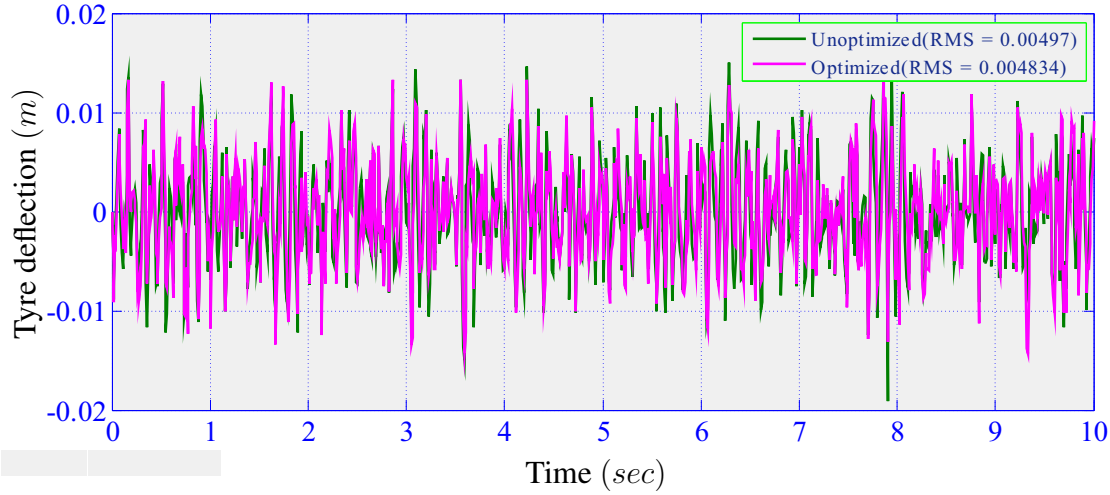

Figure 6.4: Tyre deflection of original and optimized ASS system

mass acceleration and tyre deflection comprises the comparing parameters. In Figure 6.3, the RMS value of sprung mass acceleration decreases from 1.335 to 1.275 m/s^2 by optimization. This change is -4.49%, which implies an increase of RC by 4.49%. Figure 6.4 presents tyre deflection with its RMS value. Optimization reduces RMS value of tyre deflection by 2.74% as well. This leads to an improvement of RH by 2.74%. In the results of single objective optimization there is a decrease of RMS of sprung mass acceleration from 1.335 to 0.9460 m/s^2 i.e. an increase of RC by 29.14% and an increase of RMS of tyre deflection from 0.004970 to 0.005789 m i.e. a decrease of RH by 18.51%.

Table 6.1: Comparison of optimized CSS with ASS system

		Original	Optimized	% increase of RC	% increase of RH
CSS	$a_{RMS}(m/s^2)$	1.335	1.292	3.22%	2.58%
	$td_{RMS}(m)$	0.004970	0.004842		
ASS	$a_{RMS}(m/s^2)$	1.335	1.275	4.49%	2.74%
	$td_{RMS}(m)$	0.004970	0.004834		

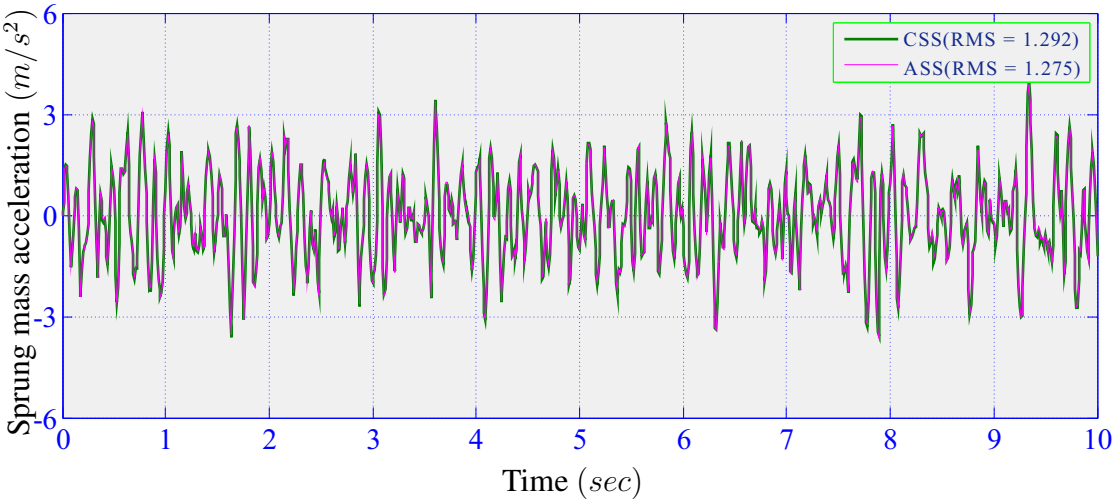

Figure 6.5: Comparison of sprung mass acceleration of CSS and ASS system

6.1.3 Comparing Optimized CSS and ASS system

Optimization affects both CSS and ASS system. The effect of optimization on the two systems is compared by sprung mass acceleration and tyre deflection. Figure 6.5 gives the sprung mass acceleration of the two systems with time. In this figure, the reduction in RMS of sprung mass acceleration is 3.22% for CSS system and 4.49% for ASS system from their original system. This clearly indicates the improvement in RC by ASS system is greater than CSS system which is by 1.27%. Another comparison is made for RH. Figure 6.6 dedicated for this comparison. In this figure, the reduction in tyre deflection is slightly higher in ASS system than CSS system. Employing optimization increases RH by 2.58% in CSS system and 2.74% in ASS system. Since a multi-objective optimization is used, it has a lower positive impact on RC and RH. A summary of the comparison is given in Table 6.1.

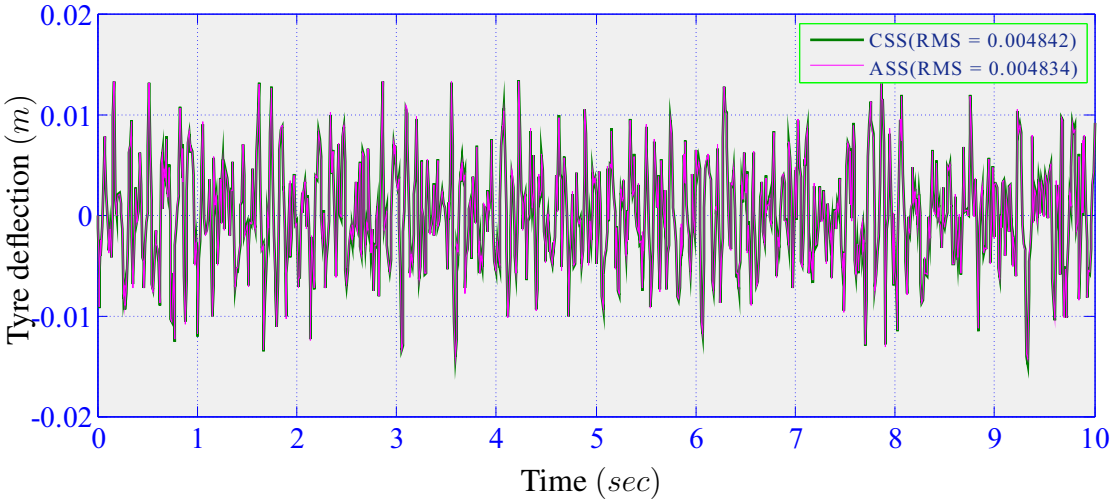

Figure 6.6: Comparison of tyre deflection of CSS and ASS system

Table 6.2: Variation of RC and RH with m_s on CSS system

№	$m_s(Kg)$	$a_{RMS}(m/s^2)$	$td_{RMS}(m)$
1	350	1.2450	0.004776
2	375	1.1600	0.004758
3	400	1.0860	0.004743
4	425	1.0210	0.004729
5	450	0.9631	0.004717
6	475	0.9114	0.004706
7	500	0.8650	0.004696
8	525	0.8230	0.004688
9	550	0.7849	0.004680
10	575	0.7502	0.004672
11	600	0.7185	0.004666

6.2 Variation of RC and RH with Sprung mass

6.2.1 Variation of RC and RH with sprung mass on CSS system

Figure 6.7 shows as sprung mass increases both sprung mass acceleration and tyre deflection decrease. Figure 6.7 is analysed to determine the RMS value of sprung mass acceleration and tyre deflection at each sprung mass value. Table 6.2 gives the RMS of sprung mass acceleration and tyre deflection at each sprung mass. in this Table, for increasing sprung mass the RMS of sprung mass acceleration and tyre deflection are decreasing. The decrease of of RMS of sprung mass acceleration and tyre deflection means the increase of RC and RH respectively.

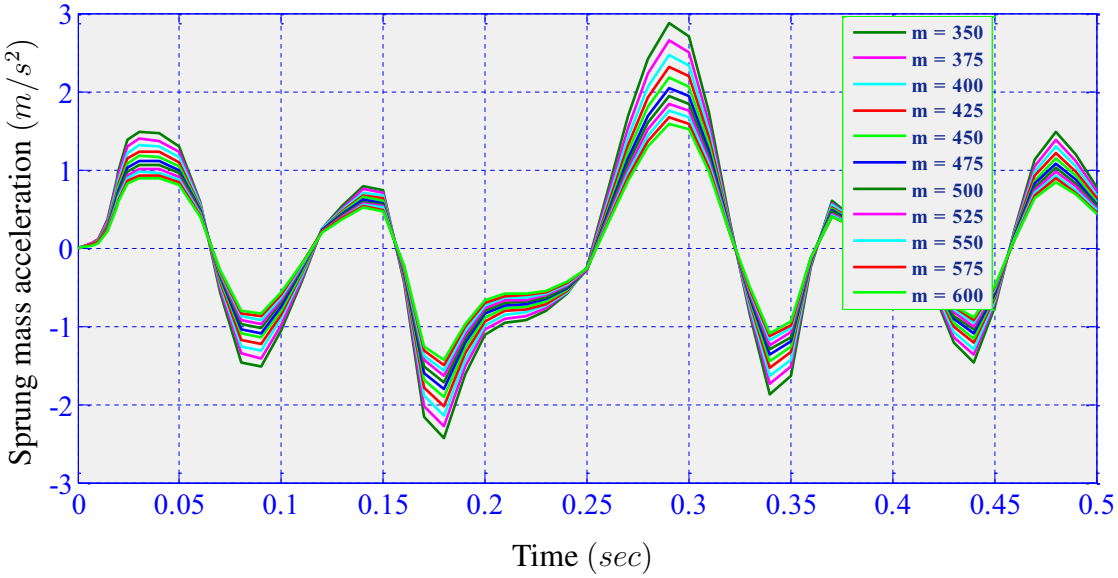

Figure 6.7: Variation of sprung mass acceleration with m_s on CSS system

Table 6.3: Variation of RC and RH with m_s on ASS system

№	$m_s(Kg)$	$a_{RMS}(m/s^2)$	$td_{RMS}(m)$
1	350	1.2240	0.004770
2	375	1.1410	0.004754
3	400	1.0680	0.004739
4	425	1.0040	0.004727
5	450	0.9472	0.004716
6	475	0.8964	0.004706
7	500	0.8508	0.004697
8	525	0.8095	0.004689
9	550	0.7721	0.004682
10	575	0.7380	0.004675
11	600	0.7067	0.004669

6.2.2 Variation of RC and RH with sprung mass on ASS system

Variation of sprung mass causes the variation in RC and RH. This is due to the variation of sprung mass acceleration and tyre deflection. In Figure 6.8, as sprung mass increases both sprung mass acceleration and tyre deflection decrease. And in Table 6.3, which is the analysed result of Figure 6.8, the RMS value of both sprung mass acceleration and tyre deflection decreases. This decrease of RMS of sprung mass acceleration and tyre deflection implies an increase of RC and RH respectively.

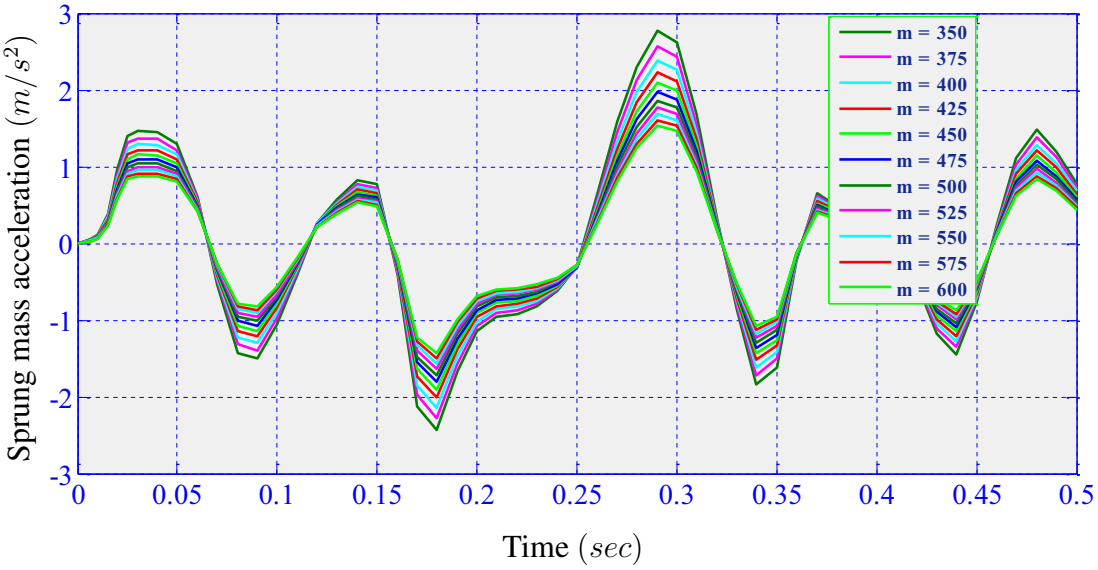

Figure 6.8: Variation of sprung mass acceleration with m_s on ASS system

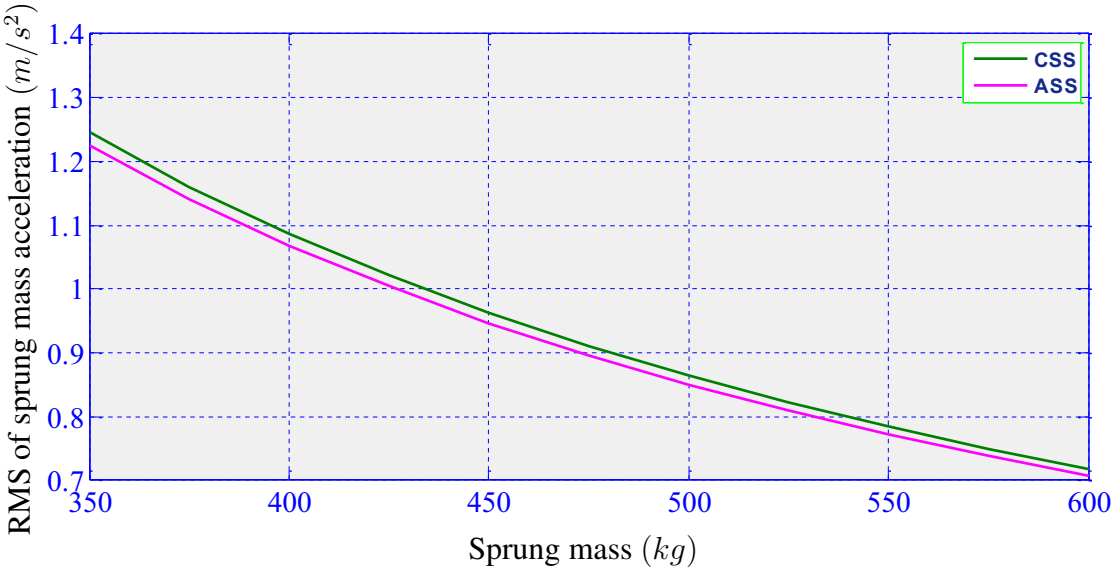

Figure 6.9: Comparison on variation of RC with m_s for CSS and ASS system

6.2.3 Comparing variation of RC and RH with m_s for CSS and ASS

In both CSS and ASS systems, increasing sprung mass has a positive effect in increasing RC and RH. The varying nature of RC is more or less similar for both CSS and ASS system, Figure 6.9. The RMS of sprung mass acceleration declines non-linearly. But the varying nature of RH is slightly different, even though the RMS value of tyre deflection declines non-linearly for both systems, Figure 6.10. In this figure, RH of CSS system is increasing slightly higher than RH of ASS system.

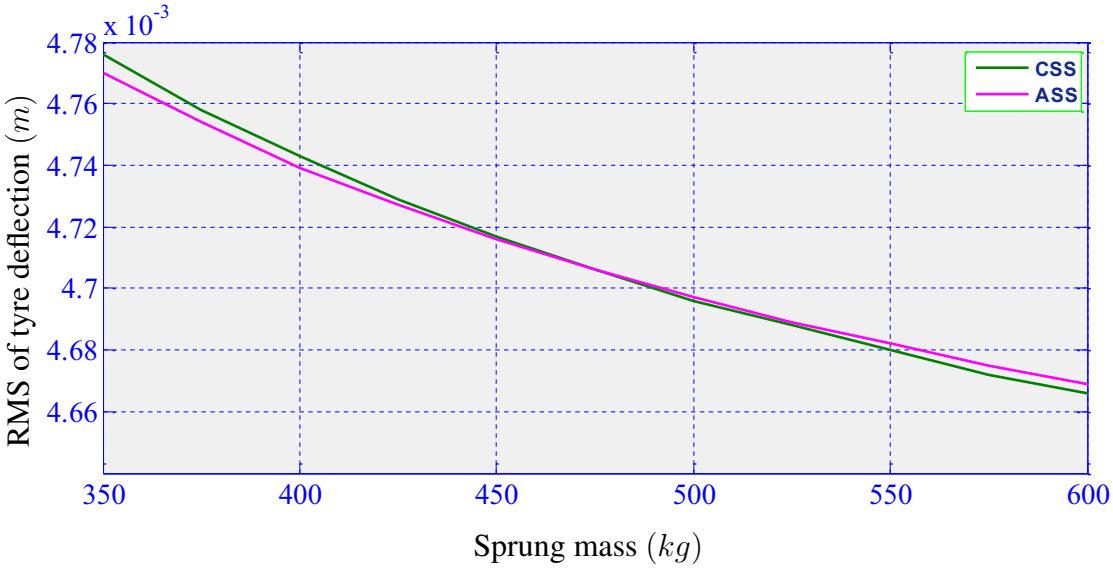

Figure 6.10: Comparison on variation of RH with m_s for CSS and ASS system

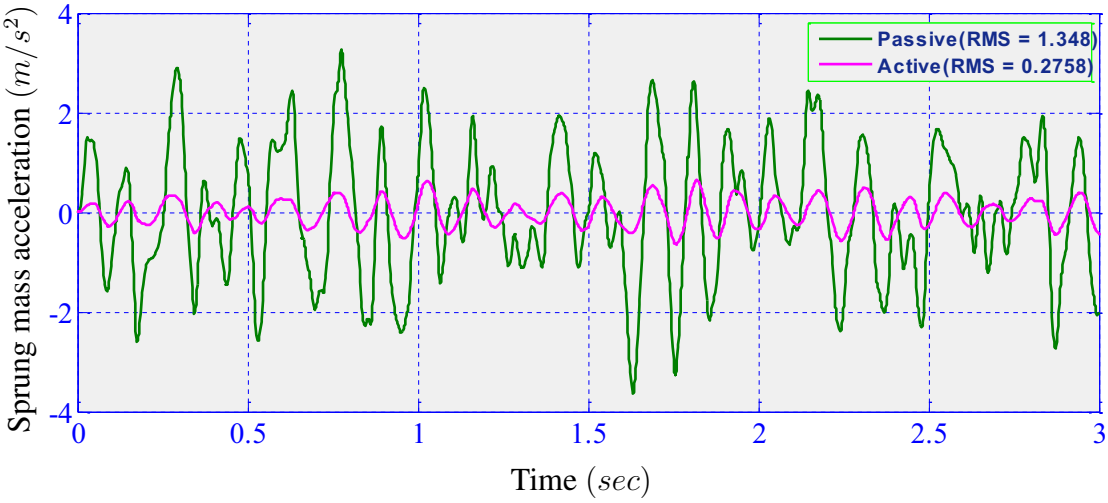

Figure 6.11: Sprung mass acceleration of passive and active CSS system

6.3 Comparing Active CSS and ASS system

6.3.1 Comparing Passive and Active CSS system

A simulation results of sprung mass acceleration and sprung mass displacement for passive and active CSS system are given in Figure 6.11 and Figure 6.12 respectively. The simulation is run for 3 seconds. For CSS system, the RMS of sprung mass acceleration decreased from 1.348 to 0.2758 m/s^2. This results an increase of RC by 79.54% because of employing FLC. It also reduces unsprung mass acceleration, sprung mass displacement and unsprung mass displacement highly.

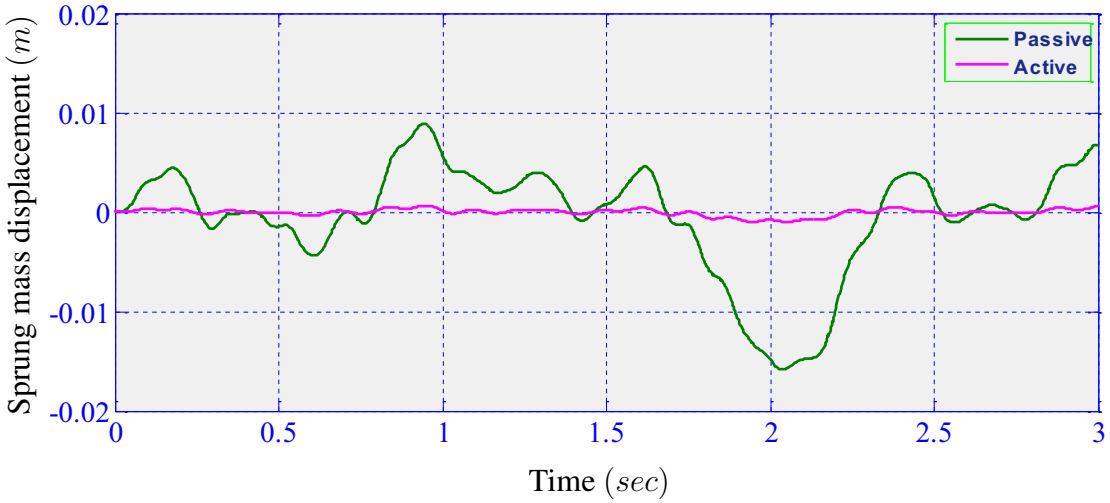

Figure 6.12: Sprung mass displacement of passive and active CSS system

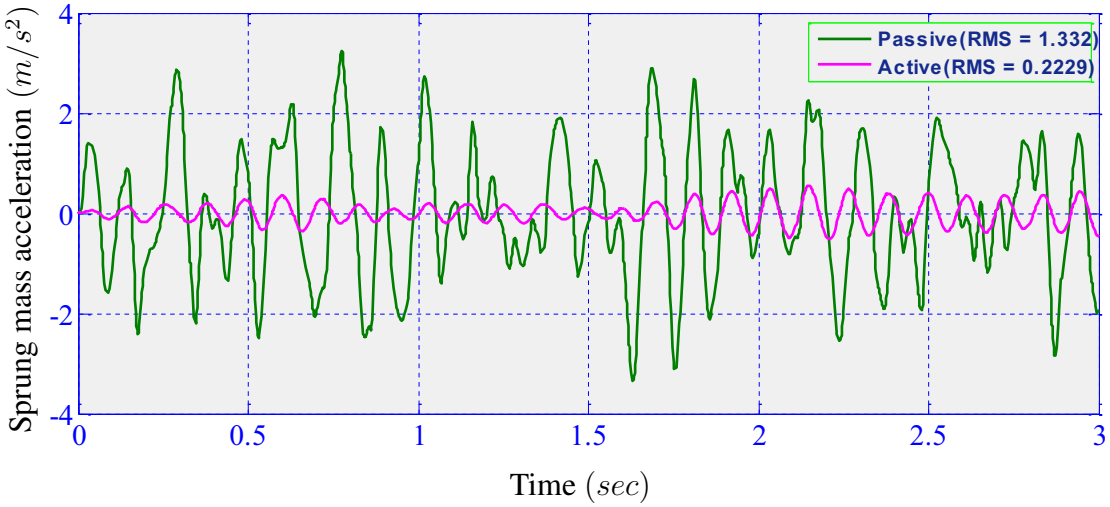

Figure 6.13: Sprung mass acceleration of passive and active ASS system

6.3.2 Comparing Passive and Active ASS system

A simulation results of sprung mass acceleration and sprung mass displacement for passive and active ASS system are given in Figure 6.13 and Figure 6.14 respectively. The simulation is run for 3 seconds. For ASS system RC is increased by 83.27% by employing FLC. It also reduces unsprung mass acceleration, sprung mass displacement and unsprung mass displacement highly.

6.3.3 Comparing Active CSS with ASS system

This is the final comparing part of the research in which active CSS system is compared with active ASS system. In Figure 6.15, sprung mass acceleration is compared between

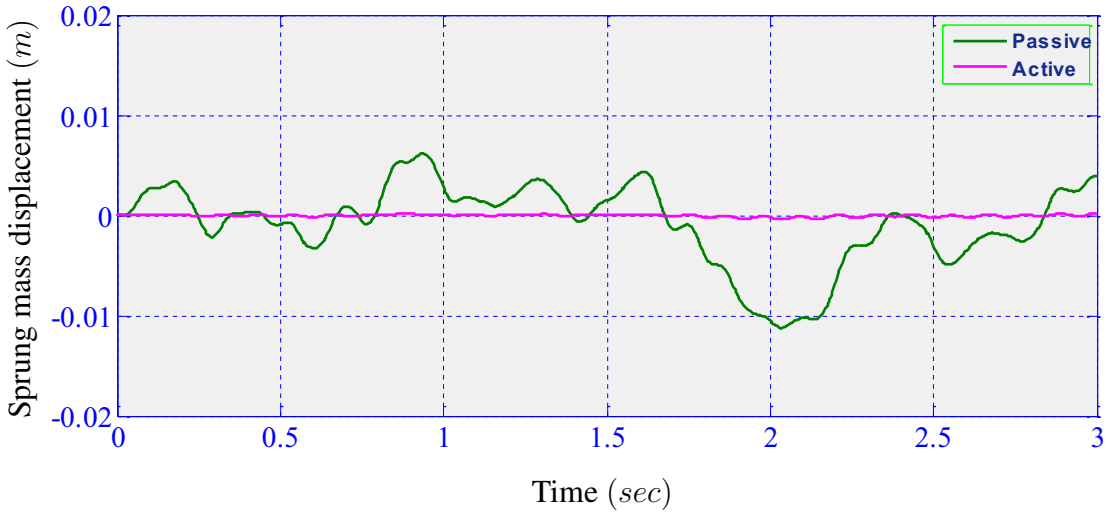

Figure 6.14: Sprung mass displacement of passive and active ASS system

Table 6.4: Comparison of CSS system with ASS system for RC

	Passive	Active	% increase of RC
RC of CSS system	1.348	0.2758	79.54%
RC of ASS system	1.332	0.2229	83.27%

CSS and ASS system. ASS system responds highly to FLC than CSS system. The use of ASS systems rather than CSS systems reduces RMS value of sprung mass acceleration from 0.2758 to 0.2229 m/s^2. As of FLC improves RC by 83.27% on ASS system and 79.54% on CSS system, the improvement in ASS is greater than that of CSS by 3.73%. This indicates that ASS system can give a better ride comfort than CSS system in the case of active suspension system. The comparison is summarized in Table 6.4. In Figure 6.16, sprung mass displacement is compared for CSS and ASS system. Sprung mass displacement is also reduced highly by using ASS system than CSS system. In addition, unsprung mass acceleration and unsprung mass displacement of ASS system is much lower than that of CSS system.

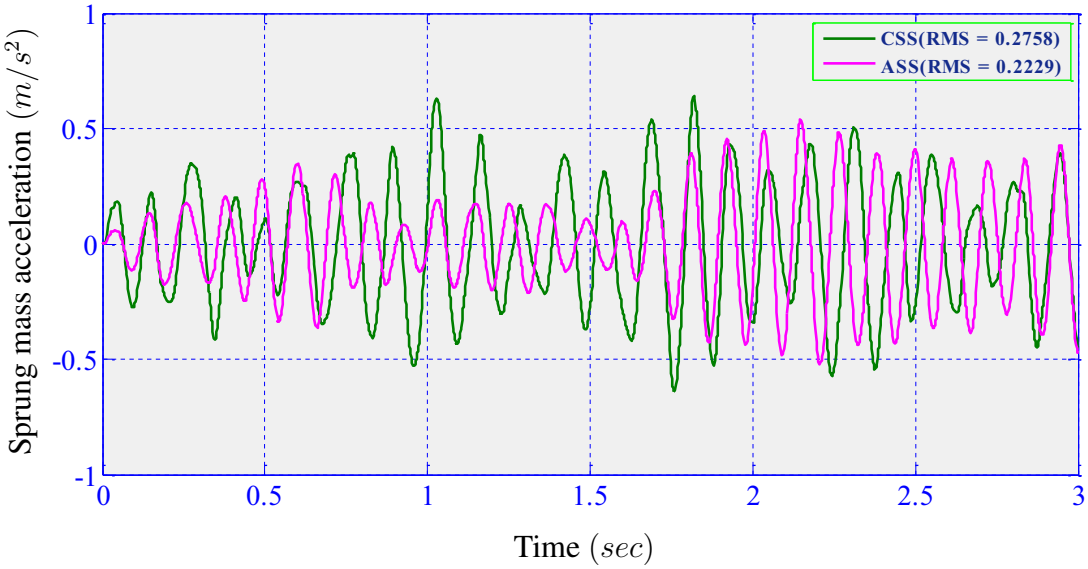

Figure 6.15: Sprung mass acceleration of Active CSS and ASS system

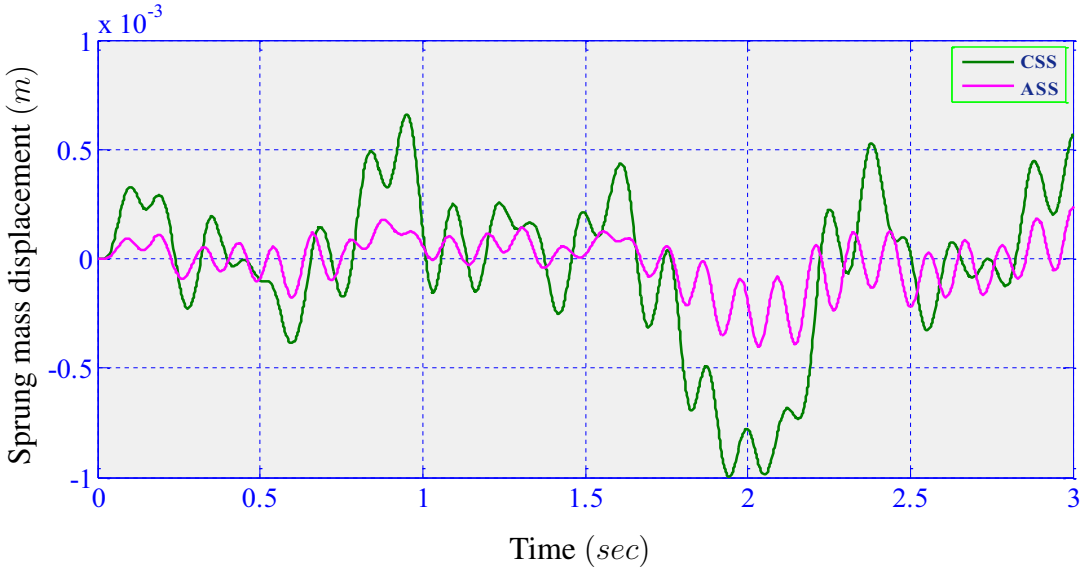

Figure 6.16: Sprung mass displacement of Active CSS and ASS system

CHAPTER 7

CONCLUSION AND RECOMMENDATION

7.1 Conclusion

ASS systems are suspension systems which use air spring between sprung and unsprung masses for vibration attenuation. There are different types of ASS systems based on their design. CSS system is the one that uses coil spring as a suspension spring. These systems are of various types depending on their design too.

The mathematical model of air spring is developed from the bases of thermodynamic on adiabatic closed system. The model is validated with a correlation coefficient of 0.9987. The air spring is used in ASS system mathematical modelling of quarter car. A mathematical model of CSS system is also developed and validated with good correlation coefficients.

Both CSS and ASS systems are optimized by multi-objective GA using MATLAB for RC and RH. CSS system improves RC by 3.22% and RH by 2.58%, whereas ASS system improves RC by 4.49% and RH by 2.74%. This means ASS system can give 1.27% more RC than CSS system and 0.16% more RH than CSS system.

The variation of RC and RH with sprung mass is also presented. In both CSS and ASS systems, the variation of RC with sprung mass has similar nature, in that it increases with the increase of sprung mass. But the nature of RH is slightly different. This is the fact that, as sprung mass increases, RH is relatively highly increasing in CSS system than ASS system.

Finally, a multi-input-single output FLC is developed in MATLAB. The FLC has 45 rules. It is integrated to both CSS and ASS system in Simulink. In CSS systems, RC is improved by 79.54% and also unsprung mass acceleration, sprung mass displacement and unsprung mass displacement are reduced in advance. In ASS system, RC is improved by 83.27%. Unsprung mass acceleration, sprung mass displacement and unsprung mass displacement are even highly reduced in ASS system than CSS system. The improvement of RC in ASS system is more than CSS system by 3.73%.

7.2 Recommendation

ASS systems have a relatively good RC and RH capability over CSS systems in light duty vehicles. They also have lesser destruction to road. Because of these, it is better to use ASS systems in light duty vehicles. But before the application of ASS systems to these vehicles, experimental verification of simulation results is highly recommended. The design of the air cylinder has to be good enough to prevent heat and pressure losses, because the results are obtained on these considerations. In fact, the losses may have the chance to alter the results. All the simulations are done in time domain analysis, it is also recommended to conduct frequency domain analysis to determine frequency nature and mode shapes.

REFERENCES

[1] A. Mitra, N. Benerjee, H. Khalane, M. A. Sonawane, D. R. Joshi, and G. R. Bagul, "Simulation and analysis of full car model for various road profile on a analytically validated matlab/simulink model," *Journal of Mechanical and Civil Engineering*, pp. 22–33, 2013.

[2] A. C. Mitra, E. Fernandes, K. Nawpute, S. Sheth, V. Kadam, and S. J. Chikhale, "Development and validation of a simulation model of automotive suspension system using msc-adams," *Materials Today: Proceedings*, vol. 5, no. 2, pp. 4327–4334, 2018.

[3] A. C. Mitra and N. Benerjee, "Ride comfort and vehicle handling of quarter car model using simulink and bond graph," in *Proceedings of the 1st International and 16th National Conference on Machines and Mechanisms, IIT Roorkee, India*, 2013.

[4] M. Zehsaz, F. Vakili-Tahami, A. Fasihi, and A. A. Majidi Jirandi, "Sensitivity of ride comfort to suspension characteristics of an off-road vehicle under road excitation," *International Journal of Emerging Technology and Advanced Engineering*, vol. 2, no. 5, pp. 422–431, 2012.

[5] A. Shirahatti, P. S. S. Prasad, P. Panzade, and M. M. Kulkarni, "Optimal design of passenger car suspension for ride and road holding," *Journal of the Brazilian Society of Mechanical Sciences and Engineering*, vol. 30, no. 1, pp. 66–76, 2008.

[6] H.-S. Tan and T. Bradshaw, "Model identification of an automotive hydraulic active suspension system," in *Proceedings of the 1997 American Control Conference)*, vol. 5, pp. 2920–2924, 1997.

[7] C. Qiu, "Analysis on simulation modeling of automobile vibration and ride performance," vol. 10, no. 21, pp. 12953–12958, 2014.

[8] G. Quaglia, M. Scopesi, and W. Franco, "A comparison between two pneumatic suspension architectures," *Vehicle system dynamics*, vol. 50, no. 4, pp. 509–526, 2012.

[9] G. S. Prassad and M. K. Mohan, "A contemporary adaptive air suspension using lqr control for passenger vehicles," *ISA TRANSACTIONS*, vol. 93, pp. 244–254, 2019.

[10] O. Demir, I. Keskin, and S. Cetin, "Modeling and control of a non-linear half-vehicle suspension system: a hybrid fuzzy logic approach," *Nonlinear Dynamics*, vol. 67, no. 3, pp. 2139–2151, 2012.

[11] A. Kruczek and A. Stribrsky, "A full-car model for active suspension-some practical aspects," in *Proceedings of the IEEE International Conference on Mechatronics*, pp. 41–45, 2004.

[12] R. Darus and Y. M. Sam, "Modeling and control active suspension system for a full car model," in *2009 5th International Colloquium on Signal Processing & Its Applications*, pp. 13–18, 2009.

[13] K. Toyofuku, C. Yamada, T. Kagawa, and T. Fujita, "Study on dynamic characteristic analysis of air spring with auxiliary chamber," *JSAE review*, vol. 20, no. 3, pp. 349–355, 1999.

[14] M. Akpakpavi and H. Jiang, "Modeling, simulation and body height adjustment control of full car laterally interconnected air suspension system," vol. 6, no. 5, pp. 31–42, 2017.

[15] H. Zhu, J. Yang, and Y. Zhang, "Modeling and optimization for pneumatically pitch-interconnected suspensions of a vehicle," *Journal of Sound and Vibration*, vol. 432, pp. 290–309, 2018.

[16] S. J. Lee, "Development and analysis of an air spring model," *International Journal of Automotive Technology*, vol. 11, no. 4, pp. 471–479, 2010.

[17] W. Li, Y. Chen, S. Zhang, E. Mao, Y. Du, and H. Wen, "Damping characteristic analysis and experiment of air suspension with auxiliary chamber," *IFAC-PapersOnLine*, vol. 51, no. 17, pp. 166–172, 2018.

[18] S. Narayan, A. S. Alsagri, and V. Gupta, "The design and analysis of hybrid automotive suspension system," *International Journal of Mechanical and Production Engineering Research and Development*, vol. 9, no. 4, pp. 637–642, 2019.

[19] V. Q. Le, "Comparing the performance of suspension system of semi-trailer truck with two air suspension systems," *Vibroengineering Procedia*, vol. 14, pp. 220–226, 2017.

[20] M. M. Moheyeldein, A. M. Abd-El-Tawwab, K. Abd El-gwwad, and M. M. M. Salem, "An analytical study of the performance indices of air spring suspensions over the passive suspension," *Beni-Suef University journal of basic and applied sciences*, vol. 7, no. 4, pp. 525–534, 2018.

[21] Y. Taskin, Y. Hacioglu, and N. Yagiz, "Experimental evaluation of a fuzzy logic controller on a quarter car test rig," *Journal of the Brazilian Society of Mechanical Sciences and Engineering*, vol. 39, no. 7, pp. 2433–2445, 2017.

[22] S. S. Rao, *Engineering optimization: theory and practice*. John Wiley & Sons, 2009.

[23] R. Likaj, A. Shala, M. Bruqi, and M. Qelaj, "Optimal design of quarter car vehicle suspension system," in *14th International Research/Expert Conference*, pp. 417–420, 2010.

[24] I. ISO, "8608: 2016 mechanical vibration–road surface profiles–reporting of measured data," *BSI Standards Publication: London, UK*, 2016.

[25] M. P. Nagarkar, Y. J. Bhalerao, G. J. V. Patil, and R. N. Z. Patil, "Ga-based multi-objective optimization of active nonlinear quarter car suspension system—pid and fuzzy logic control," *International Journal of Mechanical and Materials Engineering*, vol. 13, no. 1, pp. 1–20, 2018.

[26] I. ISO, "2631-1: Mechanical vibration and shock-evaluation of human exposure to whole-body vibration-part 1: General requirements," *Geneva, Switzerland: ISO*, 1997.

[27] Z. Chi, Y. He, and G. F. Naterer, "Design optimization of vehicle suspensions with a quarter-vehicle model," *Transactions of the Canadian Society for Mechanical Engineering*, vol. 32, no. 2, pp. 297–312, 2008.

[28] K. Rajeswari and P. Lakshmi, "Pso optimized fuzzy logic controller for active suspension system," in *2010 International Conference on Advances in Recent Technologies in Communication and Computing*, pp. 278–283, 2010.

[29] K. M. Passino, S. Yurkovich, and M. Reinfrank, *Fuzzy control*, vol. 42. Addison Wesley Longman, 1998.

[30] A. B. Tegegn, "Direct torque control of induction motor based on genetic algorithm and fuzzy adaptive pi controller," Master's thesis, Addis Abeba Science and Tecnology University, Ethiopia, 2019.

[31] A. J. Qazi, U. A. Farooqui, A. Khan, M. T. Khan, F. Mazhar, and A. Fiaz, "Optimization of semi-active suspension system using particle swarm optimization algorithm," *AASRI Conference on Intelligent Systems and Control*, vol. 4, pp. 160–166, 2013.

[32] S. G. Mirji and A. S. Arockia, "Fuzzy logic control for half car suspension system using matlab," *International Journal of Engineering Research & Technology*, vol. 3, no. 3, pp. 10–16, 2014.

[33] R. K. Pekgökgöz, M. A. Gürel, M. Bilgehan, and M. Kisa, "Active suspension of cars using fuzzy logic controller optimized by genetic algorithm," *International journal of engineering and applied sciences*, vol. 2, no. 4, pp. 27–37, 2010.

APPENDIXES

Appendix I: Optimization Tool window of MATLAB

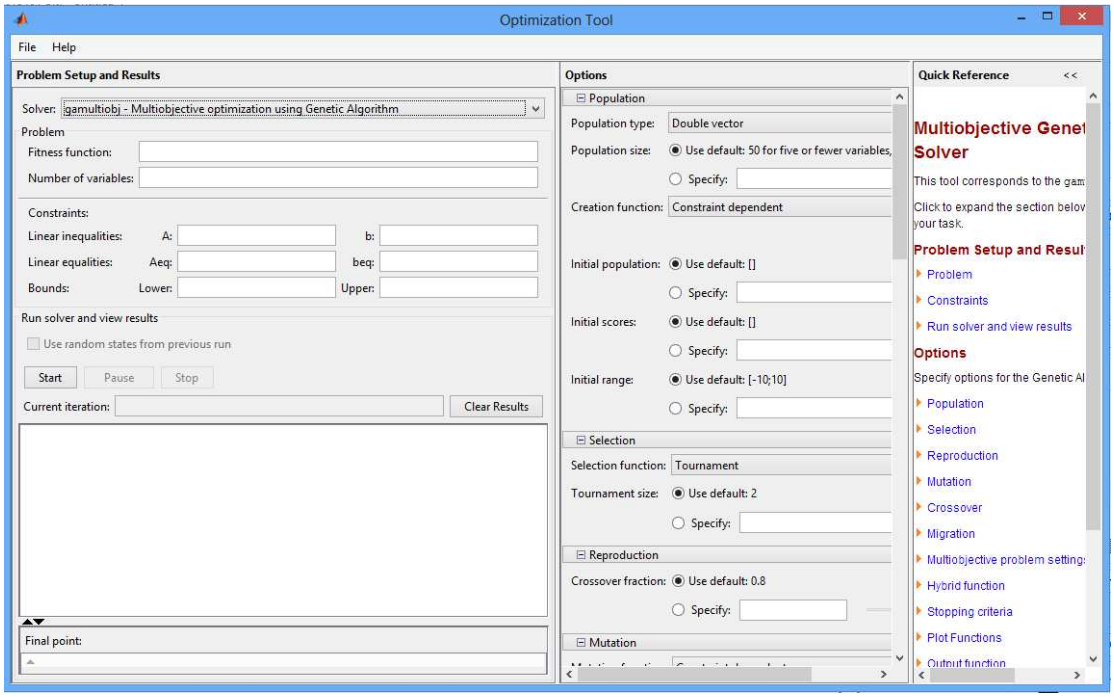

Appendix II: CSS System Optimization Process

```
function [x,fval,exitflag,output,population,score] =
CSSOptimizationResult2(nvars,lb, ub,ParetoFraction_ Data)
%% This is an auto generated MATLAB file from Optimization Tool.
%% Start with the default options
options = gaoptimset;
%% Modify options setting
options = gaoptimset(options,'ParetoFraction', ParetoFraction_
Data);
options = gaoptimset(options,'CrossoverFcn',
{@crossoverintermediate [ ] });
options = gaoptimset(options,'Display', 'off');
options = gaoptimset(options,'PlotFcns', { @gaplotpareto });
[x,fval,exitflag,output,population,score] = ...
gamultiobj(@ride_ road,nvars,[],[],[],[],lb,ub,options);
```

Appendix III: User developed function for optimization of CSS system

```
function R = ride_road(x)



R(1)=(pi*4e-6*25*(((x(2)*x(3))/(2*(350^(1.5))*((x(1))^(1/2))))
   +((400*(x(1))^2)/(2*x(3)*350^2))))^(1/2);

R(2)=(pi*4e-6*25*((((x(2))^2)*50)/(2*x(3)*(400^2)))+((400*(x(1))^2)
   /(2*x(3)*350^2))-((x(1)*x(2)*50)/(x(3)*350*400))+((x(1)*x(3))
   /(2*50*350))))^(1/2);
end
```

Where;

$x(1) = K_c$

$x(2) = K_t$

$x(3) = C$

Appendix IV: ASS System Optimization Process

```
function [x,fval,exitflag,output,population,score] =
ASSOptimizationResult2(nvars,lb, ub,ParetoFraction_ Data)
%% This is an auto generated MATLAB file from Optimization Tool.
%% Start with the default options
options = gaoptimset;
%% Modify options setting
options = gaoptimset(options,'ParetoFraction', ParetoFraction_
Data);
options = gaoptimset(options,'CrossoverFcn',
{@crossoverintermediate [ ] });
options = gaoptimset(options,'Display', 'off');
options = gaoptimset(options,'PlotFcns', { @gaplotpareto });
[x,fval,exitflag,output,population,score] = ...
gamultiobj(@ride_ roadan2,nvars,[],[],[],[],lb,ub,options);
```

Appendix V: User developed function for optimization of ASS system

```
function R = ride_roadan2(x)

R(1)=(pi*4e-6*25*((((((x(3))^2)*x(4)*x(5))/(2*((350)^1.5)*((1.4*pi)
    ^0.5)*((x(1))^0.5)*x(2)))+((400*((1.4*pi)^2)*((x(1))^2)*((x(2))
    ^4))/(2*((350)^2)*((x(3))^2)*x(5))))))^(1/2);

R(2)=(pi*4e-6*25*(((50*((x(4))^2))/(2*((400)^2)*x(5)))+((400*((1.4*
    pi)^2)*((x(1))^2)*((x(2))^4))/(2*((350)^2)*((x(3))^2)*x(5)))
    -((50*1.4*pi*(x(1))*((x(2))^2)*(x(4)))/(350*400*(x(3))*(x(5))))
    +((1.4*pi*(x(1))*((x(2))^2)*(x(5)))/(2*50*350*(x(3))))))^(1/2);
end
```

Where;

$x(1) = P_o$

$x(2) = r$

$x(3) = h_o$

$x(4) = K_t$

$x(5) = C$

Appendix VI: A Simulink model for variation of RC with m_s on CSS system

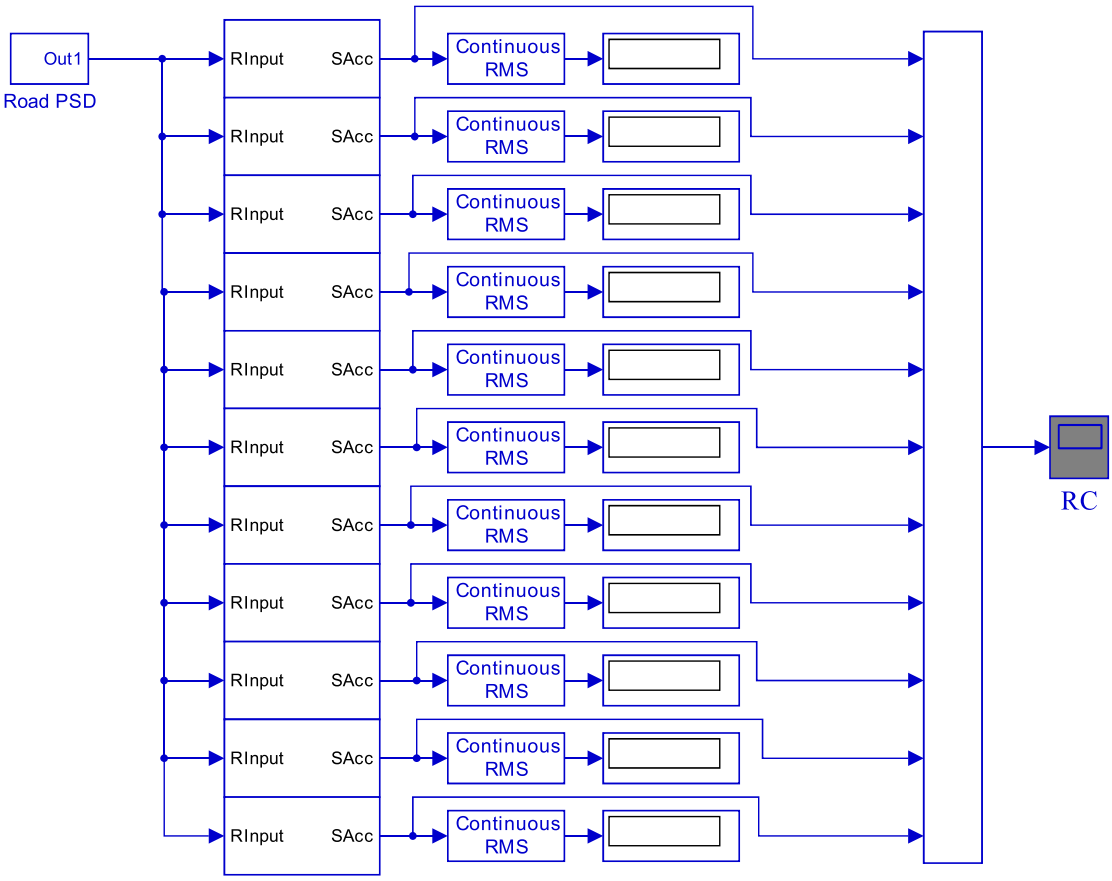

Appendix VII: A Simulink model for variation of RH with m_s on CSS system

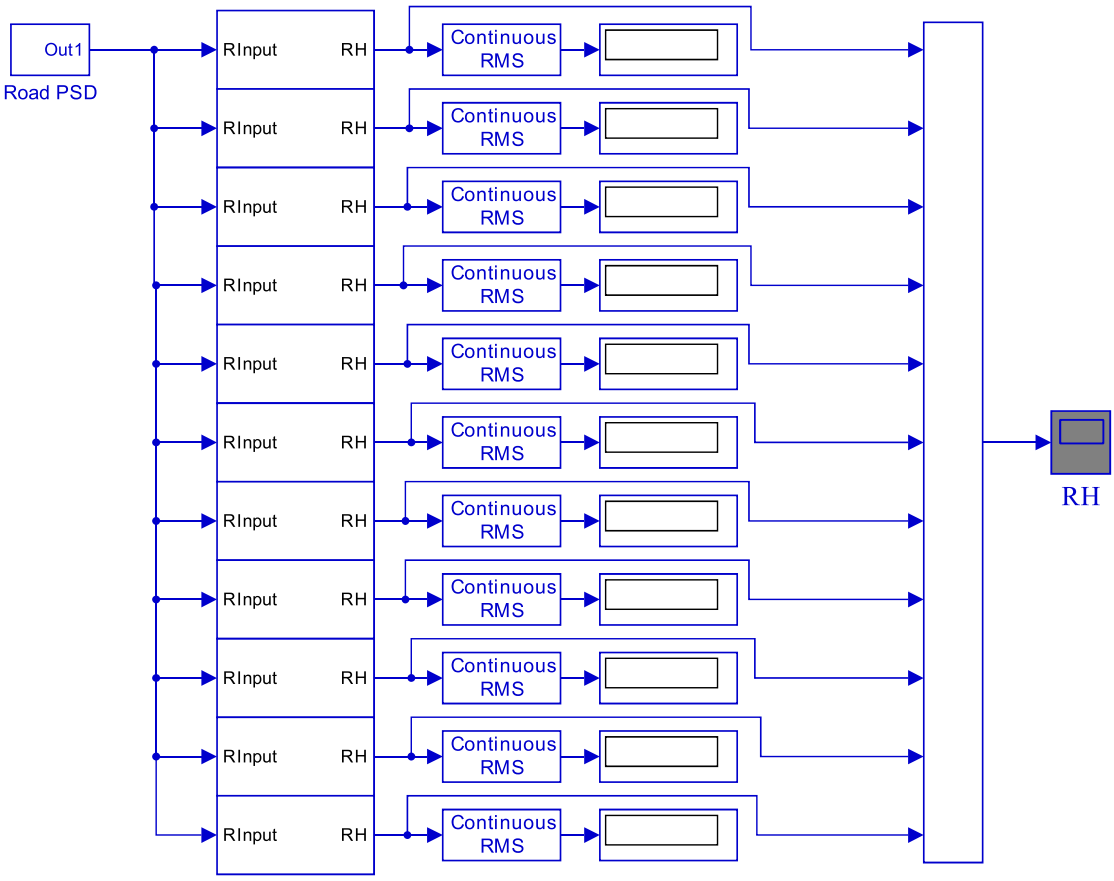

Appendix VIII: A Simulink model for variation of RC with m_s on ASS system

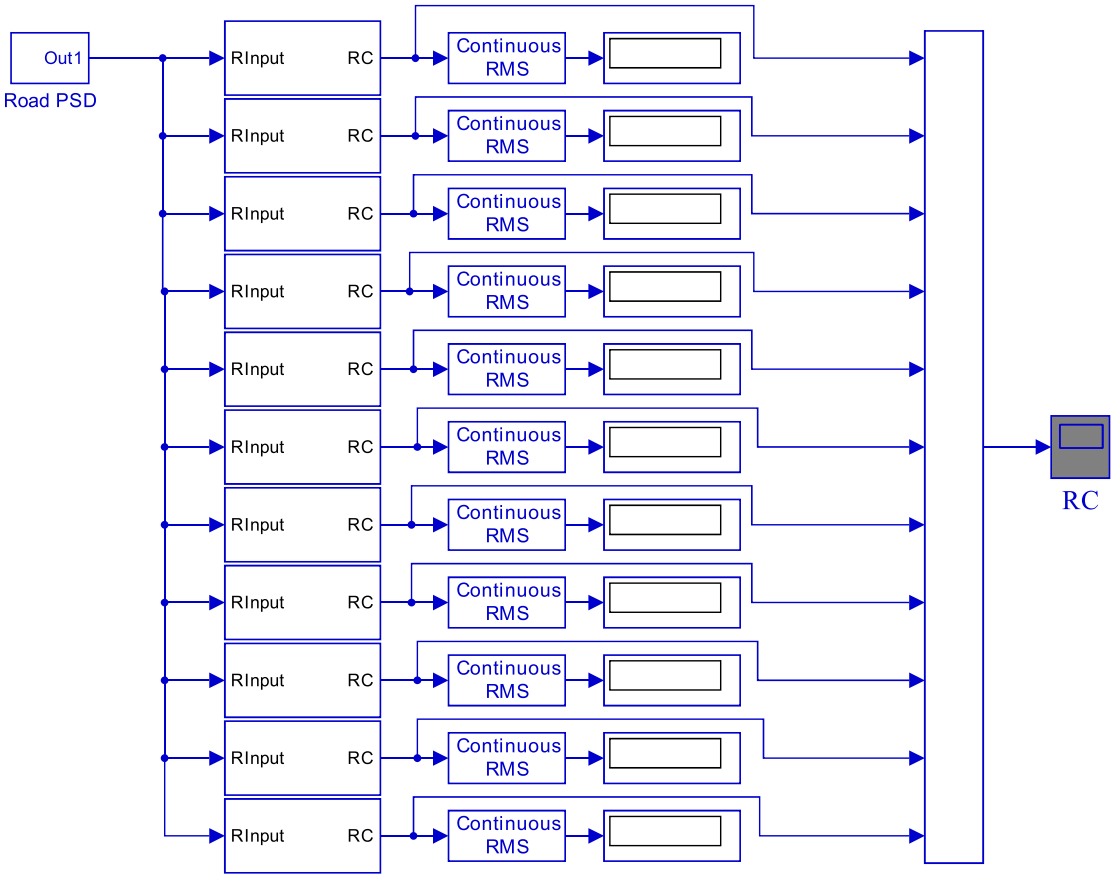

Appendix IX: A Simulink model for variation of RH with m_s on ASS system